Addis Ababa University

Addis Ababa Institute of Technology

School of Mechanical and Industrial Engineering

Design and Experimental Investigation of Improved Hybrid Solar Dryer

A Thesis Submitted to the School of Graduate Studies of Addis Ababa University in Partial Fulfillment of the Requirements for the Degree of Master of Science in Mechanical Engineering (*Thermal Engineering*)

By: Helen Worku

Advisor: Kamil Dino Adem (Ph.D.)

Co-Advisor: Sema Baye (Mr.)

Addis Ababa, Ethiopia

April, 2024

Addis Ababa University

Addis Ababa Institute of Technology

School of Mechanical and Industrial Engineering

School of Graduates Students

Design and Experimental Investigation of

Improved Hybrid Solar Dryer

This is to certify that the thesis presented by Helen Worku Kifetew, titled as “Design and Experimental Investigation of Improved Hybrid Solar Dryer” and submitted to the School of Mechanical and Industrial Engineering in the partial fulfillment of the requirements for the award of the degree of masters of science in Thermal Engineering with the regulations of the university, and meet accepted standards with respect to originality and quality.

Approved by Board of Examiners

Kamil Dino Adem (Ph.D.)	_____	_____
Advisor	Signature	Date
Abdulkadir Aman Hassen (Ph. D.)	_____	_____
Thermal Engineering chair	Signature	Date
Abdulkadir Aman Hassen (Ph. D.)	_____	_____
Internal Examiner	Signature	Date
Wondwossen Bogale (Ph.D.)	_____	_____
External Examiner	Signature	Date
Araya Abera (Ph.D.)	_____	_____ .
Dean of SMiE	Signature	Date
Sosina Mengistu (Ph.D.)	_____	_____
Director of Post Graduate Program	Signature	Date

DECLARATION

I hereby assert that the work presented is entirely my own and original. It has not been submitted for any university degree. Furthermore, I acknowledge all sources and materials used in the thesis work with utmost confidence.

Helen Worku	_____	_____
Name	Signature	Date

This thesis has been submitted for examination with the approval of a university advisor.

Kamil Dino Adem (Ph.D.)	_____	_____
Advisor	Signature	Date

ACKNOWLEDGMENT

Firstly, I thank God for support, guidance, and blessings to navigate through challenges. I am profoundly thankful to my mother, whom I regard as the Blessed Virgin Mary, for her steadfast support and I'm humbled by the inspiration from Holy saint Teklehaimanot.

I extend my deepest gratitude to my esteemed advisor, Dr. Kamil Dino, whose unwavering support and guidance have been invaluable throughout this journey. His dedicated mentorship, offered with genuine care and understanding, has empowered me to navigate challenges and pursue my research goals with confidence. I am profoundly grateful for Dr. Kamil Dino's generosity with his time, his friendly demeanor, and his unwavering commitment to my success.

I extend my special thanks to the staff members of the electrical and mechanical workshops who provided invaluable assistance. I am particularly grateful to Mr. Sema Baye, Mr. Solomon Zegeye, Mr. Masresha Wondimu and Mr. Kassaye Negash.

In the course of my academic pursuit, I owe an immeasurable debt of gratitude to my youngest, Ankion Dagmawi. Since her birth, she has shared her days with others while I pursued my studies. Despite her tender age and inability to vocalize her feelings, Ankion's silent presence has been an enduring source of inspiration and encouragement. she has guided me with a love that transcends words.

Following Ankion's silent yet profound influence, I am profoundly grateful to my husband, Dagmawi. His unwavering support and selfless sacrifices, including shouldering household responsibilities and providing financial support, have been the cornerstone of my academic journey. In addition, I extend my deepest appreciation to my mother, whose unwavering care for my children and our home has provided me with the freedom to pursue my studies without reservation.

ABSTRACT

Maintaining consistent and optimal temperature for a particular food item can be challenging when using solar food dryers, particularly when solar radiation levels are low. This issue can be mitigated by using an Improved Hybrid Solar Dryer, which has been specifically designed to address these challenges. The dryer has been experimentally investigated and compared to traditional open-air sun drying methods for drying red chilies in Addis Ababa, Ethiopia. To thoroughly analyze its performance, the system's output was measured by turning the heater on and off within the dryer for different days. The dimensions of the dryers were: 2m collector length, $2m^2$ collector area , 2.5m height of the drying chamber from the leg of the dryer to the top of chimney, A drying chamber with a length of 1 meter and a width of 1 meter was used. Each tray had an area of 0.7 square meters. The heating element had a size of 200 watts, the fan 18 watts, and the PV cell size was 4 PV modules, each with a capacity of 55 watts. Using the Improved Hybrid Solar Dryer, it took 26 hours to reach the desired moisture content of 11% from an initial moisture content of 91% on a wet basis. In comparison, open-air sun drying achieved only a 35% moisture content on a wet basis at the same 26-hour mark. The average drying rates, average collector efficiency, and average drying efficiency of the Improved Hybrid Solar Dryer with heater to reach the desired moisture content of 11% (on a wet basis) were are $0.035892\ kg/hr$, 62.3%, and 27% respectively while the average drying rate of open-air sun drying was 0.00612 kg/hr.

Keywords: Solar food dryers, Improved Hybrid Solar Dryer, Red chilies, Experimental investigation, Heater.

.

TABLE OF CONTENTS

NOMENCLATURE

a	experimental determined value, (m^3 s /kg)
$A_{d_{flat}}$	flat drying chamber floor area, (m^2)
A_{ab}	absorber surface area, (m^2)
A_c	collector area, (m^2)
A_d	drying chamber floor area, (m^2)
A_t	area of tray, (m^2)
A_v	area of the air vent (m^2),
c_p	specific heat capacity of air at constant pressure, (J/kg. K)
d	vertical distance between two adjacent trays, (cm)
d	vertical distance between two adjacent trays, (cm)
d_c	depth of collector
E	quantity of heat required to evaporate the water from chili (kJ)
H	maximum Height of hot air column (m)
h	convective heat transfer coefficient
h_{fg}	latent heat of vaporization of water (kJkg-1)
h_L	drying bed thickness (m)
I_h	annual average Incident solar radiation, (kWh/m^2 /day)
I_o	Solar constant (W/m^2).
I_T	Intensity of solar radiation incident on the plane of the collector, (W/m^2).
L_c	length of collector (m)
L_{dC}	length of drying chamber, (m),
L_t	length of tray, (m)
L_v	length of air vent (m),
ṁ	mass flow rate of drying air, (kg/s)
M_f	Final moisture content on wet basis, (%)
M_i	Initial moisture content on wet basis, (%)
M_p	mass of weight red chili, (kg)
M_r	Moisture to be removed (%)
N_t	number of trays
P	total pressure drops across the drier (pa)

P_{atm}	atmospheric pressure, (N/m^2)
P_{inlet}	pressure at inlet, (pa)
P_f	energy consumed by fan, (J)
P_h	energy consumed by the resistor, (J)
P_{outlet}	pressure at outlet, (pa)
Q	sensible heat, (KJ)
R_a	specific Gas constant (kJ/kg K)
T_a	ambient air temperature (°C)
T_c	temperature of the collector's absorber (°C)
t_d	drying time per day, (hr.)
T_f	temperature of air leaving the drying bed (K)
$t_{\max}$	maximum allowable drying temperature of chili pepper, (°C)
T_o	temperature of outgoing air from the collector, (°C)
u	superficial air velocity, (m/s)
v_a	quantity of air required in, (m^3)
v_w	Wind speed (m/s).
V_y	volume of pepper vegetable, (m^3)
W_c	width of collector (m)
W_{dc}	width of drying chamber (m)
w_{dr}	Average drying rate (Kg/hr.)
y_l	pepper vegetable crop thickness, (mm)
η_c	collector efficiency, (%)
ρ_a	density of ambient air, (kg/ m³)
ρ_s	spreading density, (kg/ m^2)
v_a	wind speed, [m/s]
$\dot{v}_a$	air volume flow rate, (m³/s)
Mi	Initial moisture content on wet basis, (%)
$Tb - Tc$	boiling and freezing temperature difference of water, (°C)
$Tdryer$	the temperature of air in the dryer, (°C)
β	dimensionless parameter
ΔP_T	gross pressure drops in the dryer (pa)
RH_{am}	relative humidity (%)

ΔP	air pressure difference, (pa)
ΔP_B	pressure drop of draying bed, (pa)
ΔP_t	total pressure drops in dryer from air heater inlet to chimney outlet, (Pa)
ΔT	temperature deference, (℃)

LIST OF TABLES

LIST OF FIGURES

CHAPTER ONE: INTRODUCTION

1.1 BACKGROUND

The practice of drying has been an age long activity since ancient times. Specifically, drying is one of the methods used for food preservation; it provides an extended shelf-life for the food items which can be spoiled within short period of times, compact (less space) and easy for transportation because of its lighter weight (Banout, 2011). Although there are so many known types of drying options, "sun drying" is the most widely used method to dry agricultural materials in developing countries.

In India, sun drying method used to dry the agricultural materials like grains, fruits and vegetables. In this activity, the crop is spread in a thin layer on the ground and exposed directly to solar radiation and other ambient conditions (mohanraj1, 2009). The direct UV rays from sun further discolored the crop and reduce the market value of crop which is dry in open sun and direct solar dryers. It is found by researchers that preservation of food by drying not only reduces wastage but it also gives better return to farmers. According to Mohana et al. (2020), open sun drying is simple and economical but suffer from many drawbacks such as no control over drying rate, over drying of crop, discoloration by UV, attack of insects and fungi, unfavorable weather etc. Farmers have dried crops in the open sun for ages, but more recently, more effective solar dryers have been developed.

(Scanlin, 1999). has reviewed that food drying was a great technique to keep the food fresh, and solar food dryers were suitable for food preservation technology. Authors concluded that every year, millions of dollars' worth of gross were lost through spoilage. Because there is no preservation of agricultural products rural farmers sell their harvested products at low rates.

Solar dryers are systems capable of harnessing the sun's energy and have been developed in different design variants such as tunnel dryers, hybrid dryers, horizontal-type and vertical type dryers, multi-pass dryers and active and passive dryers etc.(Mohana et al., 2020).

The utilization of solar energy for drying of foods remains to be attractive in terms of energy efficiency, cost-effectiveness, and rural applicability. However, a huge technological gap exists; developing low-cost and energy-efficient dryers to produce high-quality foods is a challenge. Proper design and selection of components for a solar dryer are mandatory for the effective utilization of thermal energy. Efforts is made all over world around to increase efficiency and reduce drying time thus modern dryers are equipped with fans, efficient collectors, different thermal storage materials, reflectors, auxiliary heat sources, sun tracking systems (Shrivastava, Kumar, & Baredar, 2014). In the conventional sun drying process, it takes an extended period to remove moisture from the product. On average, this process requires 3 to 4 days, even with adequate solar radiation. Furthermore, the upgraded flat plate-based solar dryers still exhibit inefficiency in terms of drying time. This inefficiency stems from the low temperature of the drying air, which hampers both the drying time and overall efficiency (Alemayehu, 2019).
Under Murali, 2019 the solar-electrical hybrid dryer (S-EHD), a supplemental/backup heating system was placed at the outlet of the solar collector to heat the air to the required drying temperature. This system would actuate automatically whenever the required air temperature was not attained in the collector, particularly during off-sunshine hours.

The improved design of the existing mechanical cabinet dryer comprises a cabinet containing trays for spreading the grains to be dried. Once the grains are loaded, the cabinet is closed, and heated air is blown across them. This heat is generated by an electrical heating coil, and a fan facilitates the movement of hot air from the heater housing to the drying chamber. Additionally, the dryer is equipped with a thermostat that automatically shuts off the machine if the inlet temperature exceeds the required value (Stephen & Emmanuel, 2009) and similar work also done in (Getahun, Delele, Gabbiye, Fanta, & Vanierschot, 2021).

Therefore, the aim of this project is to design and experimentally test a forced convection hybrid-type solar dryer using a resistance heater that is completely independent of fossil fuel or electricity dependence. This aims to elevate the air temperature inside the collector for the red chili drying process, making it suitable for applications in remote rural village farms. Additionally, this dryer will be equipped with temperature controllers to address occasional disruptions in the drying process caused by weather and climatic changes.

1.2 STATEMENT OF PROBLEM

Solar dryers rely on sunlight to function effectively. Therefore, if it's cloudy, rainy, or if sunlight varies significantly throughout different times of the year, the dryer may not perform as expected. Additionally, maintaining a steady temperature is challenging in solar dryers made to date. This can prolong drying times, potentially spoiling the product or reducing its quality. Furthermore, temperature fluctuations can lead to uneven drying, with some parts drying excessively while others remain insufficiently dried in previously constructed solar dryers.

The purpose of this project is to enhance existing dryer mechanisms by incorporating an air heater inside a collector to boost overall efficiency and speed up the drying process. Additionally, the aim is to precisely control the temperature to the required optimum level for specific food items and maintain a constant temperature until the desired moisture content is achieved, even during periods of low solar radiation. This enhanced design represents a hybrid approach to drying technology, utilizing direct solar heating of air within the collector and harnessing solar photovoltaic cells to power the resistor coil for additional heating.

1.3 RESEARCH OBJECTIVES

1.3.1 General objective

The overarching goal of this study is to design and conducting experimental investigation on hybrid solar dryer by increasing the temperature of air inside the collector and increasing the energy inside the dryer to further improve the overall efficiency of the dryer.

1.3.2 Specific objective

This research project has the following four specific objectives.

- To design a hybrid solar dryer and to make some improvements on its smartness and manageability.
- To manufacture the prototype fulfilling the design criteria.
- To conduct experiment on the new hybrid solar dryer.

1.4 SCOPE OF THE STUDY

The scope of this study encompasses the investigation and implementation of enhancements to solar dryer technology, focusing on improving efficiency and effectiveness in food drying processes. The research will include a comprehensive review of existing literature on solar drying methods and technologies, as well as an analysis of current challenges and limitations. The primary objectives of the study are to design, develop, and evaluate the performance of a hybrid solar dryer system incorporating an air heater within the collector and precise temperature control mechanisms. Methodologies will involve design, experimental testing, and data analysis to assess the impact of the proposed enhancements on drying efficiency, product quality, and energy consumption.

1.5 SIGNIFICANCE OF THE RESEARCH

This research project focuses on the design and experimental evaluation of a hybrid solar dryer that is more effective and can be quickly manufactured in large quantities for the drying of food items. If the research is successfully completed and the results are implemented, the people of Ethiopia will benefit from a rapid solar food dryer for drying their chili without using any electricity. Currently, there is no solar food dryer that operates with resistance heaters inside the collector, solely using sunlight as an energy source to speed up drying times.

1.6 LIMITATIONS

There could not be high precision enough measuring equipment available, and fixing this could be expensive. The project could take a long time to complete, and the budgeted money for dryer components' purchase could not be enough. In this instance, I could choose to use chip materials instead. Projects require various resources such as, equipment, and materials. Limited availability or insufficient allocation of these resources such as known wattage, current and voltage value of resister in Ethiopian market can hinder project quality.

1.7 ORGANIZATION OF THE RESEARCH

The first chapter describes the introduction, which includes the research history, problem statement, objectives of the research and the significance of the study. The various reviews of the research such as the theoretical and experimental reviews are covered in Chapter 2. In chapter three, the topic of materials and methodology will be covered, along with strategies for developing and conducting experiments. Chapter 4 design, Chapter 5 Experimental Analysis, Chapter 6 Results & Discussion and Chapter 7 Conclusion and Recommendations.

CHAPTER TWO: LITERATURE REVIEW

2.1 CURRENT TRENDS IN SOLAR DRYER

This study analyzes a wide range of research articles on solar energy-based drying systems and searches for any gaps in the literature that could lead to further performance improvements. Solar energy-based drying systems can bring about huge savings in fossil fuel requirements. Solar dryers are systems capable of harnessing the sun's energy and have been developed in different design variants to improve their thermal efficiency. Many variations of solar dryers have been utilized for food drying, depending on the design, materials employed during construction, the shape of the structures, energy backup systems, and auxiliary heating units are shown in the Figure 2-1. In addition, dryers are classified as direct type, indirect type, mixed type, and dryers with heat storage systems based on the incidence of solar radiation on them. Categorization into passive and active varieties based on how warm air is moved. Classification based on construction or design, such as a greenhouse dryer. Finally, hybrid sun dryers which are drying systems that combine solar drying with other heating sources or drying methods, such as forced convection systems, mechanical heat pumps, or solar assisted auxiliary thermal storage systems.

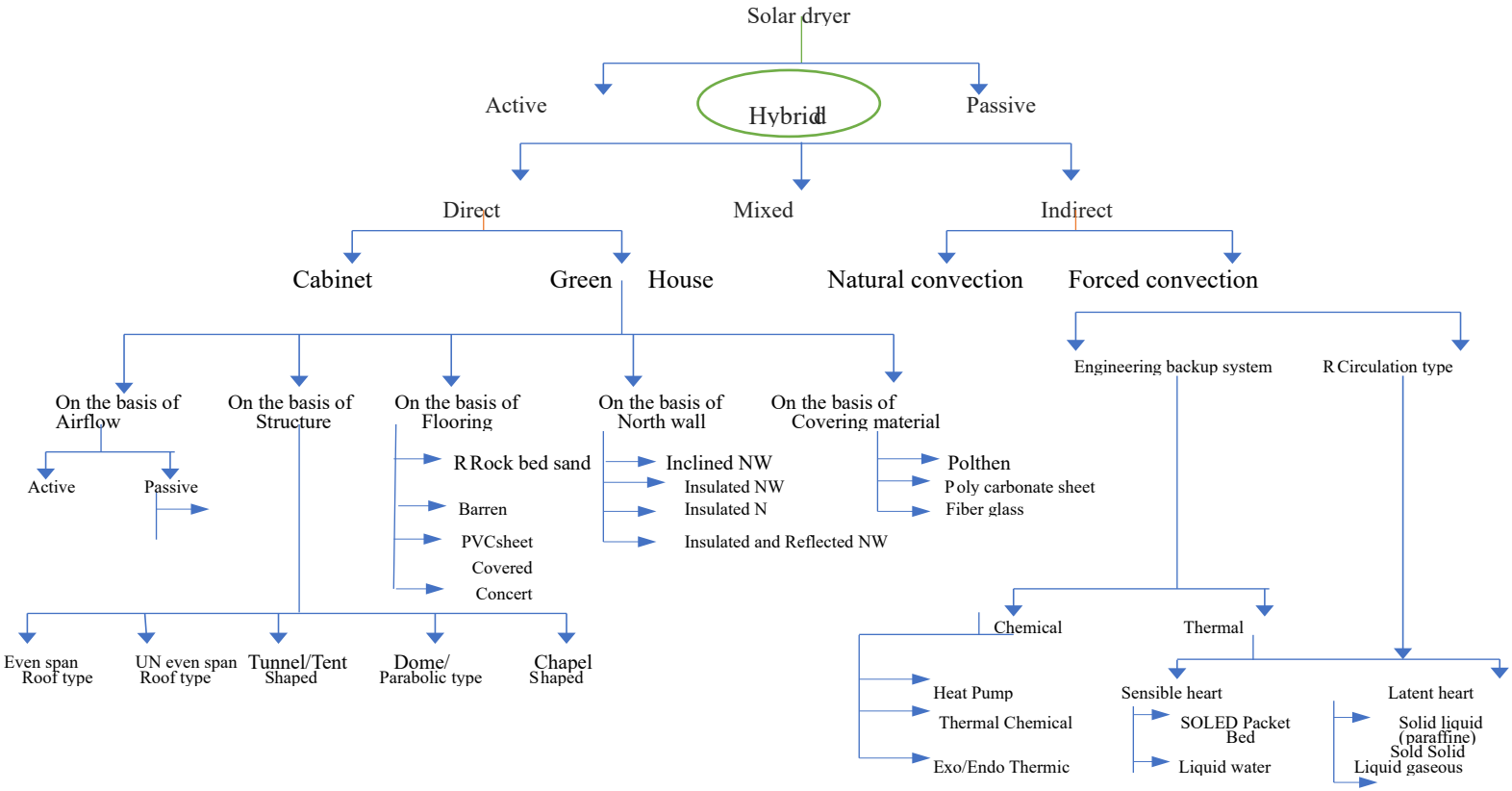

Figure 2. 1Broad classification of solar dryers (mohana et al.,2020)

The table-mounted solar tunnel dryer for drying hot and green chili's is built of a drying tunnel unit, two DC fans for air supply at the collector's inlet, a 40W photovoltaic module to power two fans, and glass wool for insulation to prevent heat loss is made and three experimental runs were carried out this are blenched solar tunnel, open sun with blanching, and open sun with traditional unblanching. Houston Texat was used to measure solar radiation, a K-type thermocouple was used to measure the temperature inside the collector, a digital meter was used to measure relative humidity and ambient temperature, an anemometer was used to measure velocity, and equations like temperature rise at the collector outlet, solar radiation regression equation were used to measure drying rate with moisture content. And Its performance in comparison to an improved and conventional dryer was conducted and found that the solar tunnel drier is technically adequate in terms of drying time, drying rate, color and pungency test. For example, the moisture content of red chili was reduced from 2.85 to 0.05 kg kg1 (db.) in 20 h, and the moisture content of green chili was obtained from 7.6 kg kg1 (db.) to 0.06 kg kg1 (db.) in 22 h in tunnel drying and 35 h to reach the moisture content to 0.10 and 0.70 kg kg1 (db.) in improved and conventional sun drying respectively (M.A. Hossain a, 2007
).

This study investigates a solar PV-powered mixed-mode solar tunnel dryer (STD) designed for drying potato chips, utilizing a flat plate solar air collector and axial DC fan to optimize thermal performance. Conducted experiments assessed drying efficiency under varying conditions, including airflow rates and treatments such as using a thermal curtain. Results indicated that the PV-powered STD reduced moisture content of potato slices to safe levels within 6 to 7 hours, demonstrating accelerated drying compared to natural methods and the products dried using this drier were of better quality as compared to their conventional sun-dried counterparts. The system achieved optimal drying efficiency of up to 34.29%, highlighting its potential for enhancing food quality and suitability for rural applications. (Eltawil, Azam, & Alghannam, 2018b)

This study Design, Development And Performance Evaluation Of Solar Dryer With Mirror Booster For Red Chilli (Capsicum Annum) presents a novel forced convection mirror booster based solar dryer designed for drying red chilli in the Malwa region of India. The dryer

integrates a single chamber for both solar energy collection and drying, enhancing efficiency while reducing costs compared to traditional systems. Experimental results demonstrate an 83% reduction in drying time compared to open sun drying, with red chillies drying from 89.09% to 4.36% moisture content in approximately 16 hours. The dryer utilizes an adjustable mirror on its glass cover to maximize solar radiation into the drying chamber, achieving a stable internal temperature about 33°C higher than ambient and The drying rate (performance estimate) in relation to the mass flow rate for solar dryer as 0.0543, 0.0622, and 0.0616 for mass flow rates of 0.456 m^3/ min, 0.285 m^3/min, and 0.002 m^3/min, respectively, with this quality were compared. The concentrator based solar dryer achieved 83% reduction in drying time when compared to that of conventional sun drying. This innovative approach not only accelerates drying but also improves the quality of dried chillies, highlighting its potential for agricultural applications in similar climates. Further research could explore scalability and broader applicability in solar drying technologies (Paul & Singh, 2013).

This study evaluates the performance of an agro-food solar dryer incorporating a photovoltaic-thermal (PV/T) air collector, developed under the European project ESSORENTREPRISE. Located at the National School of Engineering in Sfax, Tunisia, the dryer consists of two compartments: a direct solar dryer with forced convection and a mixed dryer utilizing the PV/T air collector. Tomatoes dried in this system during September 2015 demonstrated superior quality compared to natural drying methods. The PV/T collector enhances energy efficiency by converting solar radiation into both electrical power and thermal energy for air heating, significantly reducing drying time. The study underscores the potential of mixed-mode solar dryers with PV/T technology to improve drying efficiency and product quality, while highlighting the need for further research into cost-effectiveness and broader application in solar food drying technologies. (Fterich et al.).

An integrated solar drying system, featuring a collector, heat exchanger, reflector, main and additional drying chambers, and supplementary electric heaters, was developed and tested for drying chamomile in Germany during the summer of 2013. This innovative system can store solar energy in water during sunshine and reuse it during cloudy weather or at night, maintaining desired drying temperatures via a temperature controller. The main drying chamber could hold 32-35 kg of fresh chamomile, while the additional chamber held 10-12 kg. The system significantly reduced the moisture content of chamomile from 72-75% to 6% in 30-33 hours, compared to 60 hours needed to reach 9-10% moisture using open sun drying. This

represents a substantial improvement in efficiency. The Midili model was found to best describe the drying kinetics of chamomile in both chambers. The system demonstrated high efficiency by recycling 60-70% of the drying air and maintaining air temperatures between 40-50°C, which accelerated the drying process without negatively impacting the quality of the chamomile. This integrated system, which also operates with an auxiliary heat source under adverse weather conditions, shows promise for application in drying other medicinal plants, presenting a significant advancement over traditional solar food dryers (Amer, Gottschalk, & Hossain, 2022).

Thermal performance of the photovoltaic–ventilated mixed mode greenhouse solar dryer with automatic closed loop control for Ganoderma drying was investigated for its performance. Two suction fans are fixed above the door, which is driven by an electric motor of 25 w. Fans are connected to a humidity transmitter sensor that adjusted to operate the fan when the relative humidity difference between inside and outside air approaches to be the setting value. An electric heater unit is connected to a temperature controller and temperature sensor that adjusted to operate the heater unit when the inside air temperature approaches to be the setting value.
The automatically closed-loop system is used to control the relevant parameters of the drying process in the interior greenhouse solar dryer. The drying rate of the Ganoderma obtained from the greenhouse solar dryer with automatic closed-loop control is higher than that for the open sun traditional drying (Vengsungnle, Jongpluempiti, Srichat, Wiriyasart, & Naphon, 2020).

The study Drying kinetics of dried *injera* (*dirkosh*) using a mixed-mode solar dryer aimed to improve the drying process of Injera, a staple Ethiopian food, by developing a mixed mode natural convection solar dryer. The innovation lies in its design, which includes a vertical air distribution channel and a 2 m^2 collector area to enhance air circulation and uniform drying and drying chamber had a surface area of 1.5 square meters and a height of 2.2 meters, with the capacity to dry 10 kilograms of injera. This dryer reduced the moisture content of Injera from 65.5% to 12% (wet basis) within 4 hours, compared to traditional open sun drying methods. The drying efficiency and overall drying rate achieved were 17.7% and 3.69 × 10^{-5} kg/s, respectively. Midilli and Verma models were identified as the best fit for characterizing the drying kinetics of Injera. (Sileshi, Hassen, & Adem, 2021).

The study aimed to design and develop an energy-efficient solar-LPG hybrid dryer with an automatic temperature cut-off system suitable for continuous drying operations. This innovative dryer utilizes water as a thermal energy storage and heat transfer medium, integrating a flat-plate solar water collector, water storage tank, drying chamber, heat exchanger, and LPG water heater. The dryer primarily relies on solar energy during peak sunshine hours, with the LPG heater serving as an auxiliary heat source during low sunshine periods. The system demonstrated a significant efficiency, with the solar component supplying 73.93% of the heat energy while the LPG water heater supplied the remaining energy, compensating for reduced solar radiation at the beginning and end of the drying cycle. The hybrid dryer was tested using shrimps (Metapenaeus dobsoni), achieving a reduction in moisture content from 76.71% to 15.38% within 6 hours. The drying process occurred in the falling-rate period, with a maximum collector efficiency of 42.37% and a drying efficiency of 37.09%. (Murali, Amulya, Alfiya, Delfiya, & Samuel, 2020).

The study investigated the drying kinetics and quality characteristics of Indian mackerel using a solar–electrical hybrid dryer (S-EHD). Fresh Indian mackerel (Rastrelliger kanagurta) were salted and dried in the S-EHD at 45–55°C, with relative humidity of 47–62%, and air velocity of 0.60–0.80 m/s. This was compared to open sun drying (OSD). The moisture content was reduced from 61.5% to 31.8% in 8 hours using S-EHD, whereas OSD achieved a moisture content of 30.25% in 32 hours. The drying occurred in the falling-rate period for both methods, with the S-EHD showing a drying efficiency of 23.81%. The S-EHD utilized a solar flat plate air collector and a backup electrical heating system to maintain the desired temperature, ensuring continuous drying even during off-sunshine hours. Quality evaluations, including TVB-N, trimethylamine, and thiobarbituric acid analysis, indicated that mackerel dried using S-EHD had superior quality compared to OSD. Sensory analysis also favored S-EHD-dried samples for overall acceptability. The study highlights the S-EHD's effectiveness in reducing drying time and improving the quality of dried mackerel, addressing gaps in traditional solar food drying methods by incorporating controlled temperature mechanisms and hybrid energy sources (Murali, Sathish Kumar, Alfiya, Delfiya, & Samuel, 2019).

In the study on developing a hybrid portable solar tunnel dryer for peppermint, the researchers focused on enhancing efficiency by integrating a solar photovoltaic (PV) system with a flat plate solar collector. The solar tunnel dryer operates in mixed mode, utilizing both direct and indirect thermal heating, and features a thermal curtain to protect mint from direct solar

radiation. The drying performance was evaluated using single, double, and three layers of mint, and compared with open sun drying. The study found that the drying time for peppermint in the developed dryer ranged from 210 to 360 minutes, while open sun drying required 270 to 420 minutes. The daily average photovoltaic efficiency was recorded at 9.38%, while the dryer efficiency reached 30.71%, and the overall system efficiency was 16.32%. The research highlighted the importance of hybrid systems, as they mitigate the limitations of traditional solar dryers, such as dependence on weather conditions and lack of temperature control mechanisms. The study also demonstrated significant moisture reduction in the mint leaves, with drying occurring primarily in the falling-rate period. The highest drying efficiency and shortest drying time were achieved with the three-layer mint configuration. Additionally, the energy payback time was calculated to be as low as 2.06 years, and the system showed a substantial net carbon dioxide mitigation of 31.80 tons over its lifetime. This innovation is particularly beneficial for remote areas without grid connectivity, providing an efficient and sustainable solution for drying agricultural products.(Eltawil, Azam, & Alghannam, 2018a)

To determine how absorption plate design affects the evaporation rate of a solar food dryer, an optimized model with varied air heaters was designed for drying orange slices in Baghdad, Iraq, featuring four models: Model-1 with a smooth base plate and matte black aluminum absorbent plate, Model-2 with vertical fins for enhanced heat transfer, Model-3 with horizontal fins, and Model-4 with a 15 wt % silicon-coated absorber plate and vertical fins, achieving dryer efficiency enhancements of 20%, 40%, and 65% respectively compared to Model-1, demonstrating that passive enhancements such as fins and selective coatings can significantly improve solar dryer efficiency and reduce drying time (Mohammed et al., 2024).

In the drying of red pepper, a double pass solar air heater integrated with aluminum cans is used to enhance efficiency. This method employs a black-painted aluminum absorber plate coupled with aluminum can collectors. Specifically, the absorber plate measures 1 m × 2 m with a thickness of 1.25 mm and is integrated with aluminum cans that are 100 mm in length, 50 mm in diameter, and 2 mm thick. An experimental setup using this design dried 80 kg of red pepper, reducing the moisture content from an initial 79% to a final 10–12.5% on a wet basis within 50 hours. The mixed-mode double pass solar dryer achieved efficiency rates of up to 46% with aluminum can dryers, compared to 28% efficiency with conventional open sun dryers. According to the experimental results, the temperature inside the dryer chamber ranged from 30.9 to 54 °C, while the ambient temperature varied between 22.6 and 28.2 °C. This

demonstrates the effectiveness of using a black-painted aluminum absorber plate and integrated aluminum cans to enhance the performance of solar dryers, significantly improving drying efficiency and reducing drying time (Admass, Salau, Mhari, & Tefera, 2024).

In the research article "Development of a Hybrid Mixed-Mode Solar Dryer for Product Drying," a solar dryer was designed, developed, and tested at PMAS-Arid Agriculture University, Rawalpindi. The dryer was fabricated using mild steel sheets and incorporated a solar heater and three air-regulating fans. The system's performance was evaluated under various conditions. The average temperatures in the heating section and mixed-mode drying section were 65°C and 57°C, respectively, with an ambient temperature of 32°C and solar intensity of 780 W/m², all measured without load conditions. Three types of produce were dried in this solar dryer: peach (Freestone), apple (Golden), and chili (Anaheim). Fresh Freestone peaches, Golden apples, and Anaheim chilies, each weighing 10 kg with initial moisture contents of 89%, 87%, and 75% on a wet basis (w.b.), respectively, were used in the experiments. The drying times for these products ranged from 14 to 17 hours for complete drying. The final moisture content of the samples was reduced to an average of 16%, 15%, and 11% for Freestone peaches, Golden apples, and Anaheim chilies, respectively. The system demonstrated an average efficiency of 33%. Quality analysis of the dried samples, including checks on composition, total bacteria count, and color, indicated that all parameters were within the recommended quality criteria for food products (Afzal et al., 2023).

Table 2. 1 Summery of performance of solar dryers

	Performance improvement methods	Item to be dried	Performance reported quantitatively				Gaps Observed
			Efficiency (%)	Moisture content		Drying duration(h)	
				Initial In%	Final In%		
Solar PV powered mixed-mode tunnel dryer	Added PV/T air collector	potato chips	34.29	_	_	6 – 7	_
Design, Development and Performance Evaluation of Solar Dryer with Mirror Booster for Red Chili (Capsicum Annum)	with Mirror Booster	Red Chili	34.39	89.09	4.36	16	No green auxiliary heat source during off-sun shine hours
performance of an agro-food solar dryer equipped with a PV/T air collector	Use of PV/T collector	Tomatos	-	91.943	22.32	6	No green auxiliary heat source during off-sun shine hours
Integrated Hybrid Solar Drying System and its Drying Kinetics of Chamomile	store solar energy in water during sunshine and reuse it during cloudy weather	Chamomile	-	72 - 76	6	30 – 33	_
Drying kinetics of dried *injera* (*dirkosh*) using mixed-mode solar dryer	vertical air distribution channel	Injera	_	65.5	12	4	No green auxiliary heat source during off-sun shine hours and lacking a temperature control mechanism

	Performance improvement methods	Item to be dried	Performance reported quantitatively				Gaps Observed
			Efficiency (%)	Moisture content		Drying duration(h)	
				Initial In%	Final In%		
Design and Performance Evaluation of Solar - LPG Hybrid Dryer for Drying of Shrimps	ensuring continuous operation and maintaining the desired drying temperature	Shrimps	42.37	76.71	15.38	6	Use electrical energy auxiliary heat source during off-sun shine hours
Drying Kinetics and Quality Characteristics of Indian Mackerel (Rastrelliger kanagurta) in Solar–Electrical Hybrid Dryer	backup electrical heating system to maintain the desired temperature, ensuring continuous drying even during off-sunshine hours and has a temperature control mechanism	Indian mackerel		61.5	31.8	8	Not fully reliant on green energy sources
Optimized solar food dryer with varied air heater designs	fins and selective coatings	orange slices -	65	90	18	7	lacking a temperature control mechanism
Red pepper drying with a double pass solar air heater integrated with Aluminum cans	black-painted aluminum absorber plate coupled with aluminum can collectors	red pepper	46	79	10 - 12.5	50	lacking a temperature control mechanism
Development of a Hybrid Mixed-Mode Solar Dryer for Product Drying	Electrically powered solar heater and three air-regulating fans powered from an attached solar photovoltaic plate were incorporated	Anaheim chilies	33	75	11	14 - 17	Not fully reliant on green energy sources and lacking a temperature control mechanism

CHAPTER THREE: MATERIAL AND METHODS

3.1 DESIGN PROCEDURE

In the process of designing solar dryers, several factors and limitations were identified from previous literature. Additionally, pertinent data was gathered from the national meteorological service provider (EMA) based on the specific location. In cases where data was unavailable, reasonable assumptions were introduced.

Each element of the solar dryer, including but not limited to the transparent cover, absorber plate, resistance heater, storage material, fan, drying racks, chimneys, insulating material, and the covering material for the opening of the drying system, is undergoing a comprehensive assessment. This evaluation involves utilizing numerical calculations and carefully considering the selection of materials.

To further elaborate, detailed technical drawings of individual components are being generated using SOLIDWORKS software, a robust design tool. These drawings serve as a blueprint for the actual construction of the solar dryer. Once the design phase is completed, a series of tests will be carried out to ensure the functionality and efficiency of the solar dryer in real-world conditions.

3.2 SOLAR DRYER DESIGN CONSTRAINTS.

Forson Proposed additional design constraints applicable to natural /forced convection solar dryers based on previous research works to further assist in validating these dryer systems, some of which include:

Table 3. 1 Solar dryer design constraints (Forson, 1999)

For optimum performance	**Value in the range**
Length to width ratio of solar collector ($\frac{L_c}{w_c}$)	1 – 2
Maximum height of the hot air column, H	2–6-meter height variation corresponds to a total pressure range of 0.8 to 0.2.
The depth of the air channel	$\frac{1}{15} - \frac{1}{20}$ of length of the collector
The drying bed thicknesses	2.5cm

3.3 DESIGN CONDITIONS AND ASSUMPTIONS

Table 3. 2 Solar dryer design constraint

Items	Condition and assumption	Reference
Location of Addis Ababa Institute of Technology	AAiT (lat.9.04 and long.38.76)	Ethiopian Meteorological Agency
Types of products to be dried	Chili	_
Mass of weight red chili (design capacity) [kg]	4	_
Initial moisture content,M_i [%] w. b	91	Calculated value (oven method)
Final moisture content, M_f [%] w. b	11	Desired moisture content, (Zewdu, 2021) and from recommended moisture content table
Ambient air temperature, T_a [°C]	25	(Sileshi et al., 2021) and measured value
Ambient relative humidity, RH_{am}[-]	0.72	(Sileshi et al., 2021)
Maximum allowable drying temperature of chili pepper, t_{max}[°C]	65	(Getahun et al., 2020)
Drying time (sunshine hours) t_d [hrs.]	8	((Sileshi et al., 2021)
Incident solar radiation on the tilt surface [w/m^2]	390	(Tesema & Bekele, 2014) , (Sileshi, 2021) And measured value during experiment
Wind speed, v_a [m/s]	0.5	(Sileshi et al., 2021)
Collector efficiency, η_c [%]	40	Design Assumption
Vertical distance between adjacent trays, d [m]	0.2	_
Optimum PV tilt angle	11.16	(Dursun, 2021)

3.4 SIZING SOLAR DRYER

3.4.1 Moisture to be removed from chili pepper

While undergoing the drying process, moisture on the surface of the substance undergoes evaporation, and moisture from the interior moves toward the surface to participate in this evaporation.

The quantity to be dried determines the drying space, and in this case since the dryer has four trays and was for experimental purpose, an initial amount of 4 kg was to be considered for designing the dryer. Hence, chili would be dried in a batch from its initial moisture content of 91% to the desired final moisture content of 11% which is experimentally determined in (Zewdu, 2021).

The calculation of the quantity of moisture to be extracted from chili was performed using equation (1) from (Hossain, Hossain, Awal, Alam, & Rabbani, 2015).

$$M_r = \frac{M_P(M_i - M_f)}{100 - M_f} \quad (3.1)$$

$$= 4\frac{(91 - 11)}{(100 - 11)} = 3.59 \text{ kg} \approx 3.6 \text{ kg}$$

Where:

M_r = moisture to be removed (%)

M_P = mass of weight red chili (kg)

M_i = initial moisture content (%)

M_f = final moisture content (%)

3.4.2 Energy requirement

The quantity of heat required to evaporate H_2O from chills given by (JB Hussein1, 2017) , (Hossain et al., 2015).

$$E = M_p \times C_p \times \Delta T + M_r * h_{fg} \quad (3.2)$$

$$= 144 \text{ kJ} + 8136 \text{ KJ} = 8280 \text{ KJ}$$

Where:

C_p = [kJ/kg K] Specific heat capacity of chili, which is approximately 1.2 to 1.8 kJ/ kg. K (kilojoules per kilogram Kelvin) for chili. And 1.2 is taken

ΔT= [°C] temperature difference is calculated as 30°C (70°C - 40°C).

The latent heat of vaporization of water @ $100o^c$.And at a pressure of 101.3 kilopascals (kPa) is 2260 kJ/kg.

Assuming the dryer is initially at 40°C which is the outlet temperature of the collector as it is experimentally tested in (Sileshi, Hassen, & Adem, 2022) and the recommended maximum drying temperature for optimal chili processing is between 65-70°C.

3.4.3 The average drying rate of moisture

Drying rate is the amount of evaporated moisture over time (Hossain et al., 2015).

$$w_{dr} = \frac{Mr}{t_d} \tag{3.3}$$

$$= \frac{3.6\ kg}{8hr} = 0.45\ \frac{kg}{hr}$$

Where,

t_d = total drying time = 8hr.

w_{dr} = average drying rate (kg/hr.)

M_r =amount of water to be removed = 3.6kg

3.4.4 Collector area

This is the surface area of the device that is responsible for capturing and collecting solar energy. The collector area is a critical component of a solar dryer as it directly affects the efficiency and effectiveness of the drying process. The larger the collector area, the more solar energy can be captured and utilized for drying. After inserting acrylic sheet here is the manufacturing drawing and manufactured body, The daily sunshine hours during which drying can best be carried out in Addis Ababa is generally between 8am and 4pm. This implies that the useful drying hours per day is 8 hours. If the batch is to be dried for one day, the total drying hour's i.e., the drying time is 8 hrs.

Figure 3.1 Collector dimension

NASA as well as (Tesema & Bekele, 2014) stated that, the incident solar radiation in Addis Ababa is averagely 5.7 kWh/m^2/day or (233.7 w/m^2) and In Addis Ababa institute of technology average tilt angle of solar collector should be 24° for maximum exposure solar

radiation and if the collector is assumed to have an efficiency of 40%, then the area of the collector can be calculated by (Sileshi, 2014).

$$A_c = \frac{E}{I_T\, t_d\, \mu_c} \tag{3.4}$$

$$= \frac{2300 \text{ watt hour.}}{390 \text{ w/m}^2 * 8\text{hr} * 0.4}$$

$$= 1.84 \text{ m}^2 \text{ which is approximately } 2\text{m}^2$$

Where:

E [KWh] = Useful heat energy required to evaporate moisture

t_d[hr.] = Drying time.

μ_c[%] = Collector efficiency, range from 30 to 50 %.

$I_T[\text{w}/m^2]$ = Incident solar radiation on the tilt surface.

$$A_c = L_c * w_c$$

Where:

L_c [m] = Length of collector.

w_c[m] = Width of collector.

w_c =1m(assuming) (S Abubakar et al., 2018), then Lc= 2m

The absorber surface area $[A_{ab}]$ is approximately equal to the surface area of the solar collector receiving solar insolation (Abubakar et al., 2018).

Therefore, the absorber surface area becomes;

$$A_{ab} = A_c = L_c * w_c = 2m^2 \tag{3.5}$$

The air flow channel should be properly sized. The depth of the channel should be 1/15 to 1/20th the length of the collector (Scanlin, 1997). Which is 1/15 * 2m =0.13m ≈ 15 cm is taken.

3.4.5 Sizing the drying chamber Capacity and Other Dimensions

From the Design assumptions of solar dryer, the Spreading density is taken as ρ_s =1.5 kg/m^2 (Hossain et al., 2015) and the width of the collector (w_c) was considered equal to the width of the drying chamber (w_{dc}) which is equal to width of the tray in the dryer (Abubakar et al., 2018).

Therefore,

$$L_{dc} = \frac{A_d}{w_{dc}} \tag{3.6}$$

Where:

L_{dc} = [m] width of the drying chamber.

A_d = [m^2] drying chamber floor area.

w_{dc} = [m] drying chamber width.

A_c = [m] collector area.

According to (Forson, 1999) .When the ratio of the secondary to the primary Collector surface area that is $\frac{A_d}{A_c}$ is increased the overall drying efficiency increases. However, for $\frac{A_d}{A_c} > 1$.no significant difference in the performance of the dryer was observed. So, for less Consumption of material $\frac{A_d}{A_c} = 0.5$ is taken as an assumption.

Then $\frac{A_d}{2\ m^2} = 0.5 \rightarrow A_d = 1m^2$

$$L_{dc} = \frac{A_d}{w_{dc}} = 1\text{m}$$

3.4.6 Tray dimension

From (Hossain et al., 2015) tray dimensions can be calculated by:

$$A_{d_{flat}} = \frac{M_p}{\rho_s} = \frac{4\text{kg}}{1.5\text{kg}\backslash m^2} = 2.7m^2$$

where,

ρ_s Is taken as an assumption from {Hossain et al., 2015}

A_t = [m^2] tray area

Number of trays, N_t = 4

$$A_t = \frac{A_{d_{flat}}}{N_t} = \frac{2.7m^2}{4} = 0.7\text{m} \quad (3.7)$$

Hence the tray's width aligns with that of the drying chamber, initially calculated at 1 meter. However, a 0.01-meter deduction has been applied to accommodate the tray's movement within the drying chamber. Consequently, the overall width of the tray, accounting for this allowance, is 0.99 meters.

The length of tray become:

$$L_t = \frac{A_t}{W_T} = \frac{0.7\text{m}^2}{0.99\text{m}} = 0.7\text{m} \quad (3.8)$$

3.4.7 Volume of pepper vegetable crop

The volume of the pepper vegetable on the trays in the drying chamber obtained as; (Abubakar et al., 2018).

$$V_y = W_T\, L_T\, Y_l \qquad (3.9)$$

$$= 0.9m*0.8m*0.004m = 0.00288m^3$$

$$= 900mm*800mm*4mm = 2{,}880{,}000mm^3$$

Also, the total volume can be calculated by:

$$V_T = N_t\, Vy = N_t\, W_T\, L_T\, Y_l = 0.00288\ m^3 * 4 \qquad (3.10)$$

$$= 0.0115m^3 = 11{,}520{,}000\ mm^3$$

Where,

L_T = [m] Length of tray, 0.7m.

W_T = [m] Width of the tray which is equal to the width of the drying chamber.

Y_l= [m] represent how thick the pepper vegetable crop is when it is spread out in a single layer on the drying trays within the drying chamber, 0.004m.

N_t = Number of try

3.4.8 Quantity of air required

The of quantity air needed for drying (Removing the Moisture from red chili) may be estimated from the energy balance equation (Abubakar et al., 2018). The basic energy balance equation for drying process is:

$$V_a = \frac{M_r l_v R_a T_a}{c_p p_{atm} (T_o - T_f)} \qquad (3.11)$$

Where: V_a= [m³] volume of air required.

P_{atm}= [N/m^2] atmospheric pressure at a specific elevation, at Addis Ababa, Ethiopia (which is at an elevation of 2355 meters above sea level), Applying the barometric formula is 78,126.

M_r= [kg] Mass of water evaporated or moisture to be removed, 3.6

L_v= [J/kg] latent heat of vaporization of water at mean temperature, 2430,000 (latent heat of vaporization of water at 25°C)

T_a= [K] ambient air temperature, 300

R_a= [J/kg K] specific gas constant, 287

C_p= [J/kg. K] Specific heat capacity of air at constant pressure, 1005.

T_o= [K] temperature of air at the collector outlet, 316

T_f= [K] temperature of air leaving the drying bed,

The temperature of air leaving the drying bed (T_f) is calculated from the equation below

$$T_f = T_a + 0.25(\Delta T) \quad (3.13)$$

$$\Delta T = 2\beta\,(T_b - T_c)\,\frac{I_t}{I_o} \quad (3.14)$$

$$= 2*0.2(373k)\left(\frac{390}{1367}\right) = 42.56$$

$$T_f = 300k + 0.25\,(42.56)k = 306.34k$$

Where:

β = A dimensionless parameter, with values ranging between 0.14 and 0.25, was assumed to be 0.2.

$T_b - T_c = [k]$ The temperature difference between the boiling and freezing Point of water at standard atmospheric pressure and 100 o^C is taken,

I_t = [W/m^2] level of radiation reaching the surface of the collector plane.

I_o = [W/m^2] solar constant, denoted by a given value of 1367

$$\mathbf{v_a} = \frac{\mathbf{M_r\, l_v\, R_a T_a}}{\mathbf{c_p p_{atm}\,(T_o - T_f)}}$$

$$= \frac{3.59\text{ kg} * 2400{,}000\left[\frac{J}{kg}\right] 287\text{J/kg K} * 300\text{K}}{1005\frac{J}{kg\,k} * 78{,}126\text{ pa} * (316\text{K} - 306.34\text{k})}$$

$$= 945\text{ m}^3$$

The mass flow and volume flow rate of air also calculated by the following equations given by (S Abubakar et al., 2018).

The atmospheric pressure in Addis Ababa, Ethiopia, at an elevation of 2,355 meters above sea level, is approximately 78,126 (Pa)

3.4.9 The volume flow rate of air

$$\acute{\upsilon}_a = \frac{v_a}{t_d} \quad (3.15)$$

$$= \frac{945\text{ m}^3}{8\text{ hr}} = 118\ \frac{\text{m}^3}{\text{hr}} = 0.032\ \frac{\text{m}^3}{\text{sec}}$$

Where:

v_a = $[m^3]$ quantity of air required

t_d = [hrs.] (Total hrs. per day)

3.4.10 Mass flow rate of drying air

The estimated density of air in Addis Ababa at an altitude of 2,355 meters is approximately 0.839 kg/m^3.

$$\dot{m}_a = \acute{\upsilon}_a \, \rho_a \tag{3.16}$$

$$= 0.839 \frac{kg}{m^3} * 0.032 \frac{m^3}{s} = 0.026 \frac{kg}{s}$$

Where:

ρ_a = density of ambient air, 0.839 kg /m^3

3.4.11 Total height of the hot air column

The total height of the dryer from the leg to chimney is calculated with the equation given by (teshome, 2020).

$$H = \Delta P_T \frac{R_{a1}}{g\,(1/T_a - 1/T_o)Pa} \tag{3.17}$$

Where:

ΔP_T = $[P_a]$ gross pressure drops in the dryer.

R_{a1} = [J/kg K] specific gas constant, 287

T_o = [K] Temperature of air at the collector outlet, 326

T_a = [k] Temperature of ambient air, 298

G = [m/s^2] Gravitational acceleration, 9.8

P_{atm} = [Pa] Atmospheric pressure, 101325

ΔP_B = $[P_a]$ Pressure drops of the drying bed

ΔP_t = $[Pa]$ Total pressure drops across the dryer from air heater inlet to chimney outlet

The total pressure drop of the system is approximately twice the pressure drop of the drying bed. $\Delta P_t = 2\times \Delta P_B$, when all pressure drops are accounted for, experience has shown that, the gross pressure drop is about six-fold the value of ΔP_t. (Abubakar et al., 2018) .

$$\Delta P_T = 6 \times (2 \times \Delta P_B) \quad \ldots \text{ eqn (1)} \tag{3.18}$$

$$U = a\,(h_l\,\Delta P_B) \ldots\ldots\ldots\ldots\ldots \text{eqn (2)}$$

From the two equations we can have:

$$\Delta P_T = 6\times (2\times \frac{u^{*}h_L}{a}) = 2.58 \text{ pa}$$

Where:

u = [m\s] superficial air velocity.

a = [m^3s/kg] experimental determined value.

h_L= [m] drying bed thickness.

For natural convection of air through a thin layer of a crop ($hL \leq 0.2m$), the value of "a" is 0.465 m^3 s/kg (Forson, 1999). Researchers have used superficial air velocities ranging from 0.5 m/s to 1.5 m/s in natural flat plate solar dryers for chili drying (Forson, 1999).

Then inserting the values, we have:

$$H = \Delta P_T \frac{R_{a1}}{g\left(\frac{1}{T_a} - \frac{1}{T_o}\right) \text{Pa}}$$

$$= \frac{2.58 \text{ Pa} * 287\frac{J}{kgK}}{9.8\frac{m}{s^2} * \left(\frac{1}{300k} - \frac{1}{326.15}\right) * 101325 \text{ Pa}}$$

$$= 2.48\text{m} = 2.5\text{m}$$

3.4.12 Total pressure drops

Total pressure drops across the drier is calculated by the formula which is given by (Forson, 1999).

$$P = 0.00308\, g\, (t_i - t_{am})\, H \quad (19)$$

$$= 0.00308 * 9.8 \text{ m/s}^2 (53 - 25) * 2.5$$

$$= 2.09 \text{ Pa}$$

Where:

P = [Pa] air pressure

T_{am} = [o^c] ambient temperature

T_i = [o^c] Inside temperature

H = pressure head (height of the hot air column from the base of dryer to the point of air discharge)

An inter-tray spacing of 20 centimeters has been incorporated to facilitate unimpeded air circulation between the products. The trays themselves have a thickness of 4 millimeters. Consequently, a total of 1,016 millimeters (approximately 1 meter) has been allocated for the drying cabinet, specifically for accommodating the trays. This measurement does not encompass the dimensions of the chimney or the legs.

3.4.13 The thickness of the sand bed

In a solar food dryer sand bed thickness can vary depending on the specific design and purpose of the dryer However, a common recommendation is to have a sand bed thickness of around 1 to 2 inches (2.5 to 5 centimeters).

This sand bed serves as a heat-absorbing and heat-retaining medium. It helps to distribute heat evenly throughout the dryer, allowing for efficient drying of food. The sand bed absorbs solar energy during the day and releases it gradually during the night, helping to maintain a relatively stable temperature inside the dryer. Sand is often chosen for solar food dryers due to its high thermal mass, good thermal conductivity, affordability, and durability, making it as an effective heat storage material.

3.4.14 Heating element power calculation

If there is a temperature change during the process of removing moisture content, we need to account for both the heat required to change the state of the moisture (latent heat of vaporization) and the heat required to change the temperature of the air (sensible heat) (Hussein, Hassan, Kareem, & Filli, 2017)..

$$Q = M_p \times C_P \times \Delta T + M_r * h_{fg} \quad (3.20)$$

The latent heat of vaporization as it is calculated previously by:

$$E = M_r * h_{fg} = 7{,}910 \text{ KJ and} \quad (3.21)$$

The Sensible heat is given by:

$$Q = M_p \times C_P \times \Delta T \quad (!!! \text{ INVALID CITATION } !!!) \quad (3.22)$$

Where:

M_p = [kg] Mass of chilies, 4kg.

C_p = [kJ/kg K] Specific heat capacity of chili, which is approximately 1.2 to 1.8 kJ/ kg. K (kilojoules per kilogram Kelvin) for chili.

ΔT= [°C] temperature difference is calculated as 30°C (70°C - 40°C).

$$Q = M_p \times C_p \times \Delta T$$
$$= 4 \times 1.2 \times 30$$
$$= 144 \text{ kJ}$$
$$Q = M_p \times C_p \times \Delta T + M_r * h_{fg}$$
$$= 144 \text{ kJ} + 7910 \text{ KJ} = 8054 \text{ KJ}$$

$$\text{Power} = \frac{\text{quantity of heat}}{\text{time}} \quad (23)$$

Where; t is intended drying time (8hr.)

$$\text{Power} = 8054\text{kJ}/28{,}800\text{sec}$$

$$\text{Power} = 0.279 \text{ kW} \approx 212\text{W}$$

From the above calculation a heating element of approximately about 200W from pv as energy source is to be used.

3.4.14 Fan size calculation

The fan plays a crucial role in facilitating the even distribution of heat by pulling in surrounding air into the heater housing and expelling the heated air into the drying chamber.

It is essential to carefully choose an appropriate fan to ensure effective heat distribution (Holman, 1986).

$$\text{Fan horse Power } (p_f) = \frac{\text{Airflow} \times \text{pressure}}{6320 \times \text{fan efficiency}} \quad (3.24)$$

Where:

1 cfm = 4.91747×10-4 $m^3/\text{sec}-1$

Air flow is the volume of air passing through this drying chamber per unit of time. It's typically measured in cubic meters per second (m^3/s) or cubic feet per minute (CFM). The calculated volumetric flow rate value is $0.032 \frac{m^3}{sec}$ as given in equation (15) above when converting this value of the discharge to cubic foot per min (cfm) for standard fan selection then we get,

$0.032 \frac{m^3}{sec}$ = 67.8 cfm

This 12 cfm indicates that the solar dryer system is designed to have a fan with a capacity to move 12 cubic feet of air per minute through the air collector.

Pressure: it's the difference in pressure between the inlet and outlet of the fan which accounts for the resistance that the air encounters as it moves through the system.

$$\Delta P = P_{\text{outlet}} - P_{\text{inlet}} \quad (3.25)$$

Where:

ΔP = [Pa] Air pressure differential, 650 or 2.6 inch of water column.

P_{outlet} = [Pa] Pressure at the outlet of the fan

P_{inlet} = [Pa] Pressure at the inlet of the fan

Pressure at the inlet of the fan: p_{inlet} =101325 Pa (standard atmospheric pressure

Let's assume that the pressure at the outlet of the fan is p_{outlet} =100,675 Pa (slightly lower than the inlet pressure due to resistance). And most industrial fans have efficiency ranging from 70 - 85% as discussed by (Stephen, 2009) and an efficiency of 85% is taken.

$$\text{Fan horse Power} = \frac{\text{airflow} \times \text{pressure}}{6320 \times \text{fan efficiency}} \quad (3.26)$$

$$= \frac{67 \text{ cfm} \times 2.6}{6320 \times 0.85}$$

$$= 0.025\text{hp or } 18 \text{ w}$$

3.4.15 PV/modules size calculation

The 20W DC fan is expected to run approximately for 2 hours per day this is because fan start working only when temp21 (temperature sensor around resister which is what we call outlet collector temperature becomes above 70 degree Celsius. Therefore, daily energy consumption and PV Module Array sizing calculated from (Musa B. Ibrahim1, 2016) are as shown below ,

$$\text{Daily energy consumption} = \text{power x time} \quad (27)$$

$$= 20\text{W x } 2\text{hr.} = 40\text{Whrs}$$

It works roughly around 2hrs per day because it starts working only when the outlet collector temperature exceeds 65 0_c as it is described in the c^{++} program below.

The 200W heating element is expected to run for 6 hours per day. Therefore, daily energy consumption is calculated. Thus;

$$\text{Daily energy consumption} = \text{power x time}$$

$$= 200\text{W x } 6\text{hr}$$

$$= 1200 \text{ W hrs.}$$

$$\text{PV Module Array} = \frac{\text{Total dayily energy consumption}}{\text{Daily peak hours x PV correction factor}} \quad (3.28)$$

For PV Module Sizing a factor of 0.65 is reasonable.

$$= \frac{1240\text{whr}}{6\text{hr} * 0.65} \approx 300\text{w}$$

$$\text{No. of PV Module} = \frac{\text{total pv module needed}}{\text{standard pv module}} \quad (3.29)$$

$$= \frac{300 \text{ w/module}}{\frac{65\text{W}}{\text{module}}} = 4 \text{ PV module, Since a 65W}$$

PV cell is available on campus, I used the 65W/module standard and utilized four PV modules

3.5 CALCULATION RESULT

Table 3. 3 Calculation summery

Parameter		Equation	Dimension
Moisture to be removed from chilies [kg of water]		[1]	3.6
Energy required [kJ]		[2]	8280
vertical spacing between two consecutive trays [m]			0.2
Volume of pepper vegetable crop [m^3]		[9]	0.00288
Quantity of air required [m^3]		[12]	945
The ratio of drying chambers floor area to the collector surface area (A_d/A_c)			0.5
Heating element power [**w**]		[24]	200
PV module power[w]		[26]	65 / module
Air flow rate	Mass flow rate [kg/s]	[16]	0.022
	Volumetric air flow rate [m^3/s]	[15]	0.032
Collector	depth [m]	[4]	0.15
	length [m]	[4]	2
Tray	Length [m]	[4]	0.7
Drying chamber	length [m]	[5]	1
	Height [m]	[5]	1

3.6 DESCRIPTION OF SOLAR DRYER

The collector with L= 2m, W = 1m, d =0.15m, is constructed. Solar collectors are usually oriented and inclined at an angle with respect to horizontal for maximum capture of solar energy and the best thermal performance for year-round is obtained when the collector is facing south in the northern hemisphere and the optimum tilt angle is a latitude depended and can be given by Latitude of the location plus ten degrees which is (ϕ+10°) = 19º (Zewdu, 2021) and (Zemedkun, 2021). The parts of the collector chosen for this project are as follows: transparent covering, black painted absorber plate, insulating material, heat storage material, resistance heater, and an axial fan. (1) The acrylic transparent cover which is less expensive and is used to let sunlight into the collector while preventing heat from escaping; (2) 4mm thick black-painted metal (aluminum) is used as an absorber to absorb solar energy and convert it into heat and these materials' have excellent thermal conductivity. (3) Fiberglass insulating material is chosen for this project because it is inexpensive and simple to install, and because insulation for the solar collector's body is necessary to prevent heat loss to the environment. (4) Wood is employed as a sand bed positioned bellow the absorber plate, serving as holding heat storage material (sand) (5) A 200w heating element is used to further warm the air inside a collector, and it is safe to use inside a greenhouse collector. (6) An axial fan with DC 12V consumes between 10 to 18 watts of power is used to pull up the ambient air to the drying system.

The drying chamber will be constructed using galvanized sheet metal which is readily available in the workshop characterized by dimensions measuring 1 meter in width, 1 meter in length, and 2.5 meters in height from the ground floor. This chamber is equipped with 4 trays, chimneys, and a rear-facing door measuring 1 meter by 1 meter, thoughtfully designed to facilitate the loading and unloading of materials. To mitigate heat loss, the drying chamber will be outfitted with fiberglass insulation material. Food that needs to be dried is placed on wire mesh angle iron drying racks, each measuring 25 by 25 units, arranged horizontally with a spacing of 0.2 meters within a tray holder. These racks, 0.7 meters in length, 0.9 meters in width, and 0.5 centimeters in thickness will be used.

CHAPTER FOUR: CONSTRUCTION AND EXPERIMENTAL SETUP

4.1 DRYING CHAMBER

The drying chamber is constructed using galvanized steel-coated sheet metal which is readily available in the workshop, featuring a square base measuring 1000 mm by 1000 mm and standing at a height of 1000 mm. Its primary purpose is to facilitate the drying of samples efficiently. This chamber is equipped with 4 trays, chimneys, and a rear-facing door. The rear-facing door, made of acrylic sheet measuring 1000 mm by 1000mm, thoughtfully designed to facilitate the loading and unloading of materials.

Figure 4. 1 Drying chamber

Food that needs to be dried is placed on wire mesh angle iron drying racks, each measuring 700 mm in length, 990 meters in width, and 5mm in thickness, arranged horizontally at the center of the drying chamber with spacing of 200 mm within a tray holder.

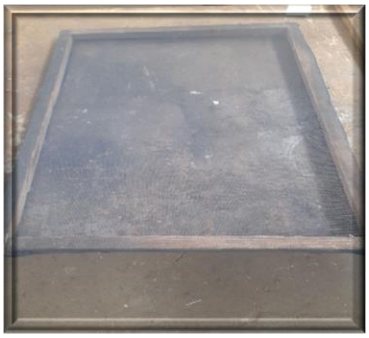

Figure 4. 2 Wire mesh angle iron drying racks

The tray holder and the framework enveloping the drying chamber, meticulously fabricated from RHS metal, ensuring a robust structural foundation that guarantees long-lasting durability. The 500mm long chimney with bottom portion that closely resembles a square pyramid has been skillfully crafted from steel-coated galvanized sheet. And A PVC cylinder is positioned on top of this pyramid-shaped base in order to optimize the structure's ventilation.

The 1000 mm-long supporting leg is located bellow the drying chamber. Its primary function is to offer solid support for the drying chambers. The hollow RHS metal is used in the construction of this structural framework ensures its strength and stability.

4.2 COLLECTOR

In the process of collecting energy and converting incoming sunlight into thermal energy solar collectors are used. These collectors form the core of food dryer design, as they are responsible for capturing and concentrating sunlight.

At the top of the collector transparent acrylic sheets is used because their transparency optimizes solar energy absorption, while their durability and UV resistance ensure long-lasting performance.

Figure 4. 3 Transparent Acrylic Sheet

a black-painted aluminum surface is chosen for them, meticulously selected for its outstanding efficiency in absorbing solar radiation. Bellow the black-painted absorber plate, strategically placed sand as a storage material.

Figure 4. 4 Black-painted aluminum

This addition further enhances the collector's performance by allowing it to store and release heat efficiently to ensure their longevity, I've constructed the collectors with galvanized steel-coated sheets on their lower part and other two sides.

Figure 4. 5. Transparent Acrylic Sheet

The dimensions of my collector measure 2000mm by 1000mm, with a depth of 200mm, providing an ideal surface area for efficiently absorbing and transforming sunlight into the heat necessary for food drying. To combat heat dissipation within the collector, thoughtfully added a layer of fiberglass material as shown in the figure.

Figure 4. 6. Transparent Acrylic Sheet

This strategic inclusion serves the crucial function of preserving and maintaining the desired temperature within the collector, ultimately contributing to the overall effectiveness of the drying process. Additionally, I added legs made of hollow RHS metal underneath the collector to hold and keep the angle in place.

The general solar collector parts combined together as shown in the figure bellow.

Figure 4.7. Result of manufactured collector

4.3 HEATING ELEMENT

A key innovation in my research is the incorporation of a 200W AC resistor wire heating element at the center of the collector (since DC is not available in the market around my location) as well as a temperature control mechanism, as illustrated in the figure below. This addition sets my collector apart from existing designs and significantly enhances its performance.

Figure 4. 8.Resistor wire heating element

4.4 SOLAR POWER SYSTEM COMPONENTS

In this study, four photovoltaic (PV) modules, each rated at 60 watts and connected in parallel, have been strategically deployed to harness solar energy. The aim is to channel this solar-generated power to operate a 200-watt AC resistor heating element and 12-volt DC axial fan.

The axial fan consumes approximately 5 watts of power, and its primary function is to facilitate the circulation of ambient air within the drying system.

Figure 4. 9. Photovoltaic (PV) modules and 12- volt DC axial fan.

To tackle the challenge of using an AC resistor obtained from the market, a solid energy management system (Solar Power System Components) set up is used. This system includes charge controller (PWM), battery, inverter, switch and Arduino making sure everything works well together.

The axial fan consumes approximately 5 watts of power, and its primary function is to facilitate the circulation of ambient air within the drying system

Charge Controller (PWM): PWM (Pulse Width Modulation) charge controller is a device that regulates the voltage and current coming from the solar panels going to the battery to the optimal levels for charging the battery. It ensures that the battery is not overcharged or over-discharged, prolonging its life.

Figure 4. 10. PWM charge controller

It is important to connect the battery first then Connect the SOLAR (PV array) next this guarantees the regulation of voltage and current. The green LED indicator will light if sunlight is present To ascertain the appropriate sizing of the Pulse Width Modulation (PWM) charge controller, the first step is to determine the necessary current capacity. This involves multiplying the number of parallel strings by the short-circuit current (I_{sc}) of each string, which is 3.63A (extracted from the information provided on the solar panel's back sticker). Considering a derating factor of 1.02 and the configuration of four parallel strings, each comprising 60W 12V solar panels wired in a plus-to-plus and minus-to-minus (parallel) arrangement, as illustrated in the above figure, the calculated current requirement then becomes 3.63 * 4 * 1.02 = 14.81A. Rounding up to the next available controller size, a 15A capacity is determined. Since all the panels are in parallel, the voltage of the array remains at 12V. Therefore, a 15A, 12V charge controller product with model KT1215 is selected as shown in technical parameters table below.

Battery: Battery stores electrical energy produced by the solar panels or another power source. It acts as energy reservoir, providing power during periods when the solar panels are not generating electricity (such as during the night or on cloudy days.

Figure 4. 11Battery

Inverter: An inverter is a device that converts direct current (DC) electricity from the battery into alternating current (AC) electricity, which is the type of electricity used in most household appliances and devices. To find the right inverter size, we need to add up the maximum power usage of both the 200W heater and two 10W fans when they're on together. And these appliances often need extra power when they start up.

Figure 4.12. Inverter

So, the inverter size should consider this extra power to handle the initial startup demands effectively, due to this the required inverter size becomes 200W +2*5W + startup demands around 300W inverter is used as shown in the figure.

Switch: A switch in this context is likely used to control the flow of electricity within the PV system. It might be used to turn the entire system on or off, or to isolate specific components for maintenance or safety reasons. The general Solar Power System.

Figure 4.13. Switch

Components combined together as shown in the figure bellow.

Figure 4. 14. Combined solar system components

To ensure precise control over the drying process within the cabinet, where a resistor functions as the heating element, it is imperative to manage both the temperature of the resistor and the rotational speed of the fan. This control mechanism is essential to prevent the drying temperature of chili from exceeding its optimal range. Achieving this control involves modulating the resistor's heat output through an on-and-off cycle while concurrently regulating the fan's operation. Specifically, the fan is activated during periods when the internal temperature of the drying cabinet is elevated, facilitating air circulation. Conversely, the fan is deactivated when the temperature within the cabinet decreases, thereby optimizing the drying conditions for the chili. This electronic system can be controlled by an Arduino.

Arduino: An Arduino is an open-source platform for electronics projects, combining a physical programmable circuit board (microcontroller) with software (IDE) running on a computer. It allows precise control of inputs or information-gathering devices such as temperature sensors, solar radiation sensors and humidity sensors and outputs or action-performing devices (fans and resistors) through code and logic tailored to user preferences. In this project, the Arduino Mega 2560 (R3) from the various Arduino families is used.

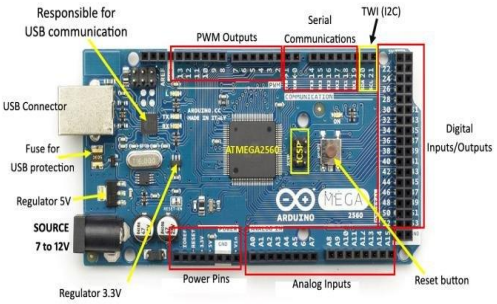

Figure 4.15. Arduino MEGA

The IDE facilitates writing and uploading code to the board. This Arduino board is a printed circuit board with some electrical components, as shown in the figure. These Arduino boards are designed for low-power applications at around 5 volts Such a connection could surpass the voltage and current limits of the Arduino, potentially causing damage. So to control high-power devices with an Arduino, using a relay is a common and appropriate solution for the safety of both the Arduino and the resistor.

A relay: is an electromechanical switch that can be controlled by a low-power signal (like the one from an Arduino) to open or close a circuit carrying a higher power load by receiving electrical signals from the fan and resistor.

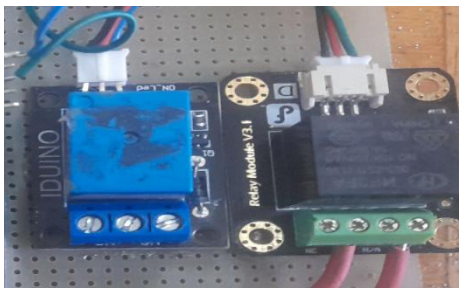

Figure 4. 16 Relay

The relay is connected to a specified pin (pin number) on the output side of the Arduino, with one side linked to the fan and resistor and the other side is battery and inverter respectively,

, while temperature sensors on the input side of the Arduino are connected via resistors to the collector and dryer, and the other side is grounded.

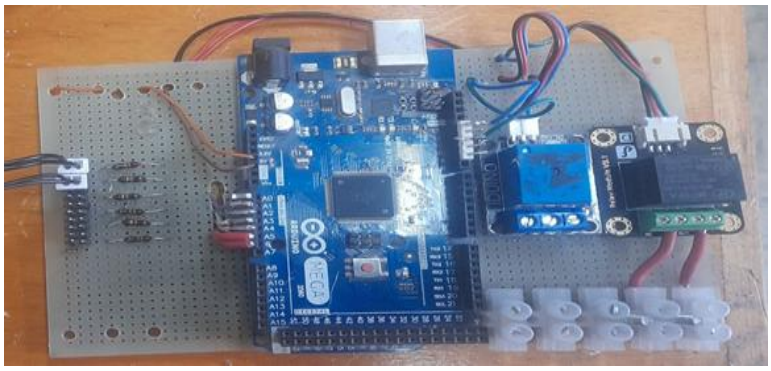

Figure 4.17. Arduino with relay board

Table 4.1. Materials Employed and design specification in the Prototype Model

Component Name	Material	Specification
Collector Cover	Acrylic sheet	2000mm x 1000mm
Absorber plate	Black painted aluminum	2000mm x 1000mm
Sand bed	Wood	2000mm x 1000mm
Dryer Support	(RHS) | Steel	RHS 25 x 25
Air Circulation Fan	_	12v, 5w
Solar Panel	_	17.6 v, 12 A. 240w
Tray with Net	Wood	550mm x 750mm
Chimney	steel-coated galvanized sheet	
Resister	_	200w
Glass fiber	_	_
Battery	_	_
Switch	_	_
Sensor	_	_
Inverter	_	300w, DC 12V To AC 220 V

Temperature Sensors: The solar drier was fitted with thermistor temperature cylinder probe sensor which was used to measure the temperatures at four different locations of trays, and four different locations of collector.

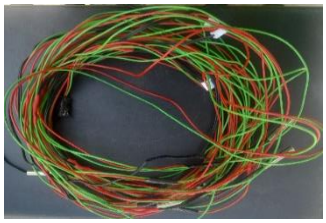

Figure 4.18. Temperature sensors

This thermistor temperature cylinder probe sensor was connected to Arduino Mega 2560 which is attached to a computer for continuous measurement of temperatures in the trays & inlet and outlet of collector. These temperatures are recorded by an Arduino & can be retrieved by computer.

A Pyranometer: The solar radiation at the position of the drier & PV module was measured by A pyranometer (Model CMP-3, Kipp & Zonen BV, Rontgenweg, Holland: accuracy 7.69 µv/w/m2) these sensors were connected to the Arduino that is simply fixed with some program software and plug in with computer

Figure 4.19. Pyranometer

Humidity: Relative humidity is measured using humidity sensors with an accuracy of (±1°C and ±1 %.) Measurements are taken at both the inlet (atmospheric) and outlet of the drying chamber and are continuously recorded and displayed with Arduino and computer respectively during the drying of red chili.

Figure 4. 20. Humidity sensors

Anemometer: Velocity of drying air was measured with a vane type heavy duty CFM thermos-anemometer (Model 407113, resolution 0.01m/s, England: Range: 0.5-40m/s, accuracy ± (2% + 0.2 m/s) at the inlet and outlet of dryer and manually recorded during the drying experiments.

Figure 4. 21. Anemometer

Electronic balance: An electronic balance with an accuracy of ± 0.1mg is used for these weight measurements. A chili was placed in each tray with its initial weight recorded, the weight is recorded at two-hour intervals to gauge the amount of weight loss.

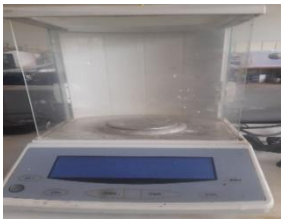

Figure 4. 22. Electronic balance

Desiccator: A container made of high-quality glass and equipped with a powerful vacuum pump is used to prevent and maintain the moisture level of chili, preserving it for the next day.

Figure 4.23. Desiccator

Hot air oven: It utilizes hot, dry air to eliminate moisture from materials or equipment. The temperature inside the oven is controlled by a thermostat, which maintains a constant temperature by turning the heating element on and off as needed. This ensures that the items inside the oven are not overheated.

Figure 4.24. Hot air oven

MB45 Moisture Balance: The MB45 Moisture Balance is a reliable moisture analyzer known for its accuracy and precision. It uses a halogen heating element to dry the sample and calculate the moisture content based on weight loss.

Figure 4.25. Moisture analyzer

Table 4.2. Experimental Instruments with application and resolution

Instrument	Application	Resolution	Range
Solar Radiation Sensor	Measures incoming solar radiation intensity.	N/A	0-2000 W/m²
Temperature Sensors	Monitor temperature inside the dryer.	0.1°C	-20°C to 150°C
Humidity Sensors	Measure humidity levels within the dryer.	1% RH	0-100% RH
Anemometer	Measures wind speed and direction (if needed).	0.1 m/s	0-50 m/s
Thermocouples	Monitor temperature at specific locations.	0.1°C	20 °C - 1300°C
Solar Tracker	Adjusts the dryer's orientation for optimal sun exposure.	N/A	N/A
Weighting Balance	Used to measure the Weight of chili	N/A	N/A
Controller	Manage and control the operation of a system.	N/A	N/A
Arduino board	Used for programming and interfacing with other electronic components.	N/A	N/A
Relay	Uses an electromagnet to mechanically operate a switch	N/A	N/A
USB cable	Used to connect electronic devices for data transfer and power supply.	N/A	N/A
Moisture Meter	Measure the moisture content of chili	N/A	N/A

CHAPTER FIVE: SETUP PROCEDURES AND IMPLEMENTATION

5.1 ESTABLISHMENT AND EXAMINATION LOCATION FOR THE DRYER SETUP

The variability of solar radiation intensity is contingent upon seasonal changes and the tilt angle of the collector. This tilt angle, in turn, is directly influenced by the specific latitude of the location. For optimal periodic tracking of solar collectors throughout the year, the following are the recommended tilt angles: $\emptyset + 25°$ for November, December, and January; $\emptyset + 15°$ for February, September, and October; $\emptyset - 15°$ for August; $\emptyset - 25°$ for May, June, and July; and $\emptyset$ for March and April as given by (Oloketuyi S Idowu*, 2013).

In the context of this thesis, based on the testing conducted between late October and early November, it is advised to implement a tilt angle ranging from $\emptyset + 15°$ to $\emptyset + 25°$ for the optimal performance of the solar drying system. Additionally, the solar drier should be strategically positioned facing south with an East-West orientation. Again Tilt Angle of Solar Panels in degrees from vertical for Addis Ababa, Ethiopia during the specific time frame of the study conducted at the end of October and the beginning of November is 81°, as evidenced by the findings published in the paper by (Salih, 2023).

Figure 5.1. Manufactured dryer wth test location

The program used which is the Arduino Mega is compatible with the Arduino software and is equipped with the ATmega2560, which is preloaded with a bootloader. This bootloader facilitates the uploading of new code without the need for an external hardware programmer. Communication is established through the original STK500 protocol, additionally, an alternative method involves programming the microcontroller directly through the ICSP (In-Circuit Serial Programming) header, bypassing the bootloader.

5.2 BLOCK DIAGRAM

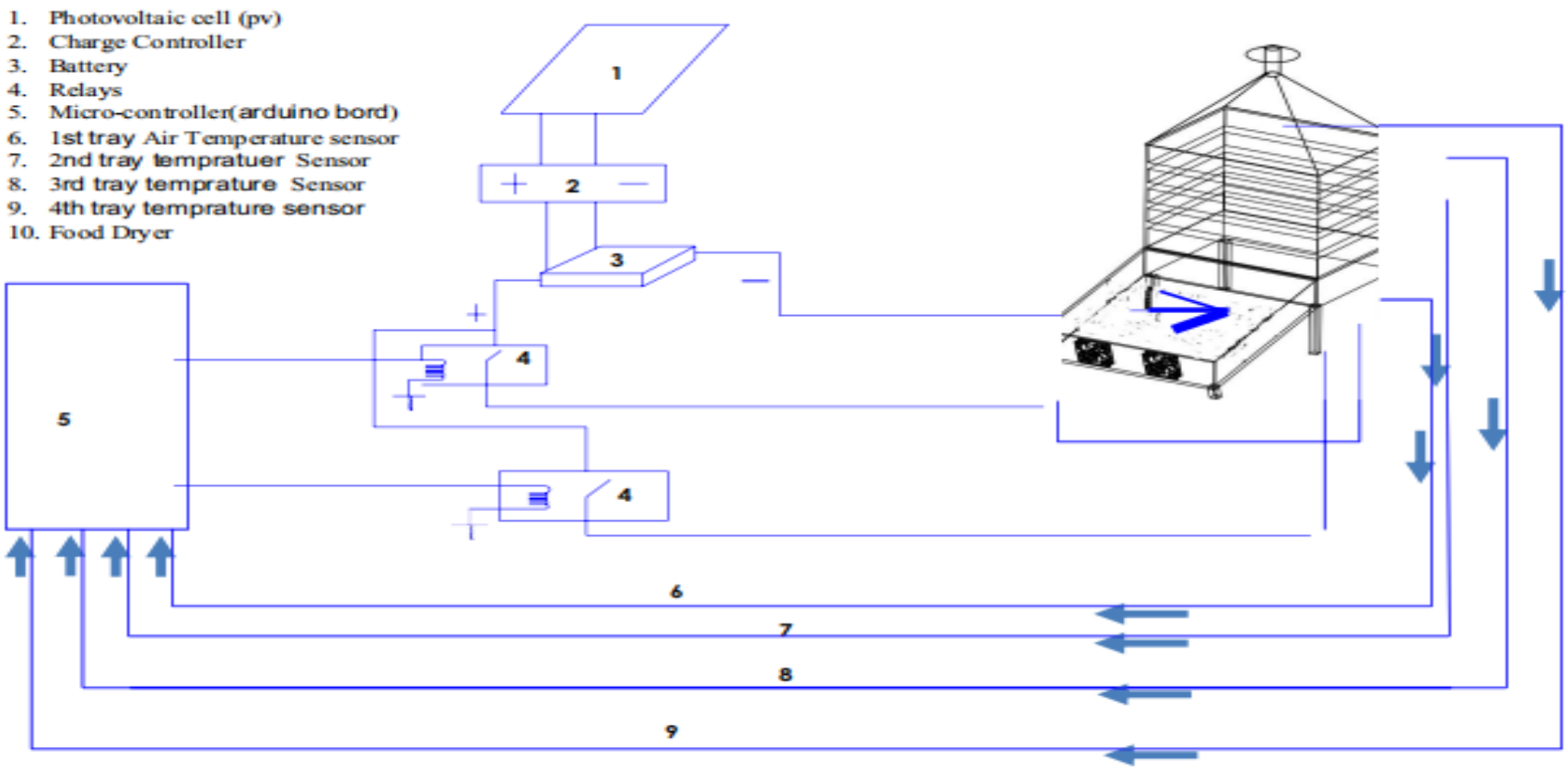

Figure 5.2. block diagram

5.3 PROGRAM FOR READING SENSORS VALUE WITH ARDUINO

```
#include <math.h>
#include <DHT.h>
#define DHTPIN 2
#define DHTTYPE DHT11
DHT dht (DHTPIN, DHTTYPE);
int Solar_rad_val;
int chk;

float hum;
#define RELAY1 13
#define RELAY2 11
int Solar_radiance =A0;
Const int therm0 = A1;
Const int therm1 = A2;
Const int therm2 = A3;
Const int therm3 = A4;
Const int therm4 = A5;
const int therm5 = A6;
Const int therm6 = A8;
const int therm7 = A9;
 float vout;
void setup ()
{
  Pin Mode (Solar_radiance, INPUT);
  dht.begin ();
  PinMode (RELAY1, OUTPUT);
  PinMode (RELAY2, OUTPUT);
  Serial.begin (9600);
}
void loop () {
 Solar_rad_val = analog Read (Solar_radiance);
  int solar_Rad= 0.00847*Solar_rad_val*100;
  hum = dht.readHumidity();
  int therm_val0;
  double Vo0, therm_res0, therm_res01,therm_res02, temp0,T0, temp01;
  therm_val0 = analogRead (therm0);
  Vo0 = ( (therm_val0 * 5.0) / 1023.0 );
  therm_res0 = ( ( 5 * ( 10.0 / Vo0 ) ) - 10 );
  therm_res01 = therm_res0 * 1000;
  therm_res02 = log (therm_res01);
  temp0= ( 1 / ( 0.001025793869 + ( 0.0002509890735 * therm_res02 ) (* therm_res02
* therm_res02 * therm_res02 ) ) );
  temp01 = temp0 - 273.15;

  int therm_val1;
  double Vo1, therm_res1, therm_res11,therm_res12, temp2,T1, temp11;
  therm_val1 = analogRead (therm1);
  Vo1 = ( (therm_val1 * 5.0) / 1023.0 );
  therm_res1 = ( ( 5 * ( 10.0 / Vo1 ) ) - 10 );
  therm_res11 = therm_res1 * 1000;
  therm_res12 = log (therm_res11);
  temp11= ( 1 / ( 0.001025793869 + ( 0.0002509890735 * therm_res12 ) + (
0.00000001149105902 * therm_res12 * therm_res12 * therm_res12 ) ) );
  temp2 = temp11 - 273.15;
```

```
  int therm_val2;
  double Vo2, therm_res2,therm_res21,therm_res22, temp20,T2, temp21;
  therm_val2 = analogRead (therm2);
  Vo2 = ( (therm_val2 * 5.0) / 1023.0 );
  therm_res2 = ( ( 5 * ( 10.0 / Vo2 ) ) - 10 );
  therm_res21 = therm_res2 * 1000;
  therm_res22 = log (therm_res21);
  temp20= ( 1 / ( 0.001025793869 + ( 0.0002509890735 * therm_res22 ) + (
0.00000001149105902 * therm_res22 * therm_res22 * therm_res22 ) ) );
  temp21 = temp20 - 273.15;

  int therm_val3;
  double Vo3, therm_res3,therm_res31,therm_res32, temp30,T3, temp31;
  therm_val3 = analogRead(therm3);
  Vo3 = ( (therm_val3 * 5.0) / 1023.0 );
  therm_res3 = ( ( 5 * ( 10.0 / Vo3 ) ) - 10 );
  therm_res31 = therm_res3 * 1000;
  therm_res32 = log (therm_res31);
  temp30= ( 1 / ( 0.001025793869 + ( 0.0002509890735 * therm_res32 ) + (
0.00000001149105902 * therm_res32 * therm_res32 * therm_res32 ) ) );
  temp31 = temp30 - 273.15;

  int therm_val4;
  double Vo4, therm_res4,therm_res41,therm_res42, temp40,T4, temp41;
  therm_val4 = analogRead (therm4);
  Vo4 = ( (therm_val4 * 5.0) / 1023.0 );
  therm_res4 = ( ( 5 * ( 10.0 / Vo4 ) ) - 10 );
  therm_res41 = therm_res4 * 1000;
  therm_res42 = log (therm_res41);
  temp40= ( 1 / ( 0.001025793869 + ( 0.0002509890735 * therm_res42) + (
0.00000001149105902 * therm_res42 * therm_res42 * therm_res42 ) ) );
  temp41 = temp40 - 273.15;

  int therm_val5;
  double Vo5, therm_res5,therm_res51,therm_res52, temp50,T5, temp51;
  therm_val5 = analogRead (therm5);
  Vo5 = ( (therm_val5 * 5.0) / 1023.0 );
  therm_res5 = ( ( 5 * ( 10.0 / Vo5 ) ) - 10 );
  therm_res51 = therm_res5 * 1000;
  therm_res52 = log (therm_res51);
  temp50= ( 1 / ( 0.001025793869 + ( 0.0002509890735 * therm_res52 ) + (
0.00000001149105902 * therm_res52 * therm_res52 * therm_res52 ) ) );
  temp51 = temp50 - 273.15;

    int therm_val6;
  double Vo6, therm_res6,therm_res61,therm_res62, temp60,T6, temp61;
  therm_val6 = analogRead (therm6);
  Vo6 = ( (therm_val6 * 5.0) / 1023.0 );
  therm_res6 = ( ( 5 * ( 10.0 / Vo6 ) ) - 10 );
  therm_res61 = therm_res6 * 1000;
  therm_res62 = log (therm_res61);
  temp60= ( 1 / ( 0.001025793869 + ( 0.0002509890735 * therm_res62 ) + (
0.00000001149105902 * therm_res62 * therm_res62 * therm_res62 ) ) );
  temp61 = temp60 - 273.15;
 int therm_val7;
  double Vo7, therm_res7,therm_res71,therm_res72, temp70,T7, temp71;
  therm_val7 = analogRead (therm7);
  Vo7 = ( (therm_val7 * 5.0) / 1023.0 );
```

```
  therm_res7 = ( ( 5 * ( 10.0 / Vo7 ) ) - 10 );
  therm_res71 = therm_res7 * 1000 ;
  therm_res72 = log(therm_res71);
  temp70= ( 1 / ( 0.001025793869 + ( 0.0002509890735 * therm_res72 ) + (
0.00000001149105902 * therm_res72 * therm_res72 * therm_res72 ) ) );
  temp71 = temp70 - 273.15;
if(temp2 > 45 )
{
 digitalWrite (RELAY1, HIGH);
}
if (temp2 < 45)
  {
  digitalWrite (RELAY1, LOW);
  }
if (temp21 < 60 && temp31 < 60)
  {
 digitalWrite (RELAY2, HIGH);
}
  if (temp21 > 70 && temp31 > 70)
  {
  digitalWrite (RELAY2, LOW);
  }
  Serial.print ("Humidity: ");
  Serial.print (hum);
  Serial.print ("\t");
  Serial.print ("Solar_rad: ");
  Serial.print (solar_Rad);
  Serial.print ("\t");
  Serial.print ("Coll_Temp1: ");
  Serial.print (temp01);
  //Serial.print ("C ");
  Serial.print ("\t");
  Serial.print ("Coll_Temp2: ");
  Serial.print (temp61);
  //Serial.print ("C ");
  Serial.print ("\t");
  Serial.print ("Coll_Temp3: ");
  Serial.print (temp71);
  Serial.print ("\t");
  Serial.print ("Coll_Temp4: ");
  Serial.print (temp2);
  Serial.print ("\t");
  Serial.print ("Drier_Temp1: ");
  Serial.print (temp21);
  Serial.print ("\t");
  Serial.print ("Drier_Temp2: ");
  Serial.print (temp31);
  Serial.print ("\t");
  Serial.print ("Drier_Temp3: ");
  Serial.print (temp41);
  Serial.print ("\t");
  Serial.print ("Drier_Temp4: ");
  Serial.print (temp51);
  Serial.print ("\n\n");
  Delay (1000);
```

5.4 TESTING AND PERFORMANCE EVALUATION

The experiment was conducted over a period of 24 days, starting from February 5th and ending on February 29th. The tests were carried out under varying weather conditions at AAiT, Addis Ababa, Ethiopia, located at latitude 9.04 and longitude 38.76. The experiments were conducted with and without a load and a heater, specifically without a heater on February 20th. Later, tests with a load and a heater were conducted from February 21st to February 29th. The experiment underwent several changes in timing due to unfavorable weather conditions, like bad weather and other obstacles. We are able to conduct tests of up to 6 hours on February 23rd and 24th, where we monitored the system from 10:00 a.m. to 4:00 p.m., on February 21st, tests were done from 12:00 PM to 4:00 PM for 4 hours and on February 22nd, from 11:50 AM to 1:50 PM, totaling 2 hours Similarly, the tests on February 27th and 28th were carried out from 1:30 PM to 4:30 PM, with each experiment lasting for 3 hours. On February 29th, the final experiment was conducted from 12:30 PM to 2:30 PM, lasting 2 hours. And a total of 26 hours it takes until the desired moisture content is reached in the solar dryer.

In this experiment the hourly temperatures of air into the collector at 4 equally spaced locations from inlet (ambient) to outlet of the collector and at 4 various passions of trays, solar insolation, temperature from the chimney outlet, humidity, as well as the wind speed were measured.

5.4.1 Performance Evaluation

The evaluation of solar dryer efficiency and effectiveness in drying food items involves analyzing parameters such as solar collector efficiency, drying rate, percentage moisture loss, and drying efficiency, as discussed by Abubakar (2018), Sileshi (2020), and Zewdu (2021).

5.4.1.1 Percentage Moisture Loss

The usual method for determining the moisture content in a product involves calculating it as a percentage, considering the weight of water relative to the weight of dry matter present. Following the equations provided by Hossain (2015) above.

$$.M_r = \frac{M_P(M_{i-} M_f)}{100- M_f} \times 100$$

5.4.1.2 Average Drying Rate

The quantity of moisture removed from the food item over the drying time and it can be determined from the equations suggested by Abubakar et al., 2018. As given in equation (3.3)

$$w_{dr} = \frac{m_r}{t_d}$$

Where:

w_{dr} = [kg/ hr.] average drying rate.

m_r = [kg] is mass of water evaporated.

t_d= [hr.] overall drying time.

5.4.1.3 Solar Collector Efficiency

The efficiency of a solar collector is the ratio of heat gained by the air leaving the collector to the incident solar energy over a particular time period [9]. The steady state thermal efficiency of the solar collector is given by (S. Abubakar et al., 2018).

Collector Efficiency (%) $$\mu_c = \frac{\dot{m}\, c_p (T_o - T_a)}{A_c\, I_t} \quad \text{.....(30)}$$

Where:

I_t= [w/m^2] total solar radiation incident on the top surface.

T_a= [°C] ambient air temperature

T_o= [°C] temperature of outgoing air from the collector

$\dot{m}_a$ = [kg/s] Mass flow rate of air

5.4.1.4 Dryer Efficiency (system efficiency)

The drying efficiency is the ratio of total heat energy required to the total heat energy supplied by the dryer to remove the moisture from the material (Leon et al., 2002), (Murali, 2019).

Drying efficiency (%) $$\mu_d = \frac{E_{req}}{E_{sup}}$$

Where: E_{req} is the total heat energy required to remove the moisture in the material (kJ) (heat energy required to raise the sensible heat + latent heat to remove moisture) and E_{sup} is the total heat energy supplied to the dryer (kJ) (heat energy received on solar collector + heat energy supplied by electrical coil). As given by (Murali, 2020)

Drying efficiency (%) $\mu_d = \frac{M_r * h_{fg}}{I*A*P_f + P_h}$ ..... (31)

Where:

μ_d = efficiency of dryer

M_r = [kg] mass of evaporated water from chili

h_{fg}= [J/kg] Latent heat of vaporization of water

I = [w/m^2] hourly average solar radiation on the aperture surface

A_c = [m^2] total energy collection surface area of the dryer

P_f = [J] energy consumed by fan

P_h = [J] energy consumed by the resistor

t_d = [s] drying time per day

To determine the initial moisture content the chili was inserted into the MB45 Moisture Balance and left until all of the moisture content was removed. This was detected by a lack of change in number in moisture balance screen, which indicated that the moisture content had stabilized at 91%. It is known that the initial moisture content of the chili was also 91%.

To determine the moisture loss and the time required to reach that moisture loss, the hot air oven method is used. Through the weight reduction calculation, an electronic balance with an accuracy of ± 0.1mg was used to weigh the chili. And chili weighing 10.88 gram initially was subjected to a drying process in oven at a temperature of 65°C (optimal chili drying temperature) then the weight of the chili was measured repeatedly with different time intervals until it reached a point where safe storage moisture content is attained. The oven drying weight reduction and moisture loss measurements are shown in the table below.

Table 5.1. Chili Moisture Reduction Data by Time using oven method

Time	Weight (gram)		
	Dish [W_1]	Chili weight reduction with time increment	Dish + chili [W_2]
8:00:00 AM	50.9	10.88 = W_S	61.86
1:00:00 PM	50.9	3.86	54.8
2:30:00 PM	50.9	2.74	53.65
4:30:00 PM	50.9	1.3	52.3
From 12:30:00 PM-4:30:00PM	50.9	1.26	52.2

$$\% \text{ moisture loss} = \frac{w_s-(w_2-w_1)}{w_s} * 100 \text{(oven method)} \ldots\ldots\ldots (34)$$

$$= \frac{10.88-(52.2-50.9)}{10.88} * 100 = 88\ \%$$

The initial moisture content of the chili was 91% as measured by MB45 Moisture Balance, after being in the oven for 12 hours, 88% of the moisture was removed as shown in figure.

Figure 5.3. Chili oven Drying Process

5.4.2 Testing material preparation

The test started by taking the weights of the chilies and place them within four trays inside the dryer and one tray exposed to direct sunlight. Take three chilies from each place (5), including Four trays inside dryer and one in the open sun, mark them as w_1, w_2 and w_3 as shown in the figure bellow. This will help me to distinguish each chili weight reduction at any time, once marked the chilies, spread them out on four trays and open sun. To keep everything organized and distinguish where the chilies are taken and place them back after weighing, take plastic bags for each try and open sun and mark with marker.

Figure 5.4. Chili Drying Methods.

CHAPTER SIX: RESULT AND DISCUSSION

6.1 VARIATION OF SOLAR INTENSITY WITH TIME

The results of the Design and Experimental Investigation of Improved Hybrid Solar Dryer performance evaluations are given in the following figures below:

Figure 6 shows a variation of solar radiation with time at 20th/02/2024 and 21th/02/2024 the maximum solar insolation recorded was 872 W/m² @ 20th/02/2024 and the minimum was 220 W/m² @ 21th/02/2024.

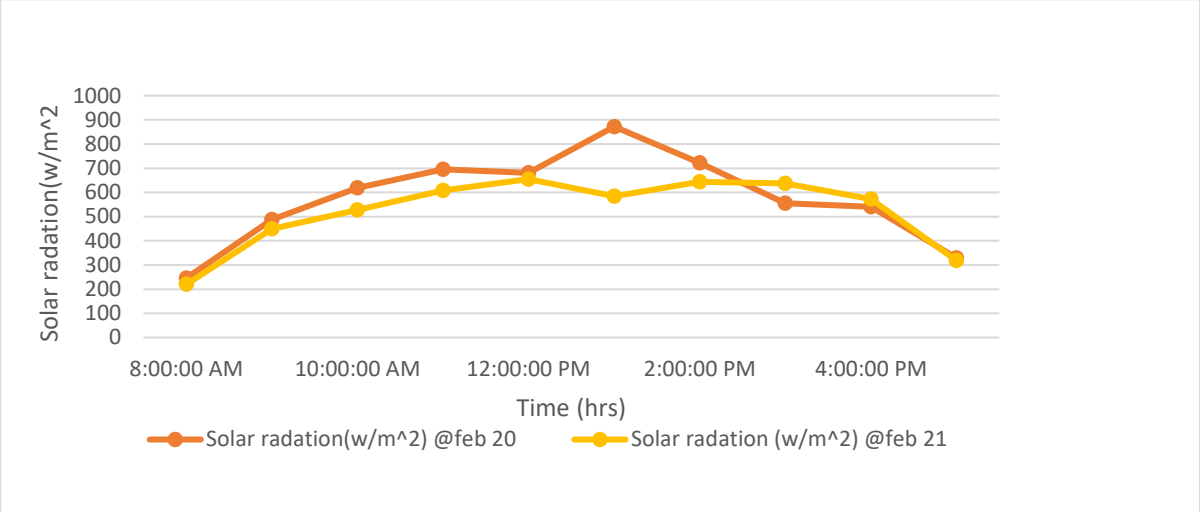

Figure 6.1. Variation of solar radiation with time at 20th/02/2024 and 21th/02/2024

6.2 VARIATION OF SOLAR INTENSITY AND COLLECTOR AIR TEMPERATURE WITH TIME

As shown in the figure bellow, between 10:30 AM and 1:30 PM, we observed a consistent increase in collector outlet temperature. However, this rise wasn't perfectly linear. The deviation from linearity occurred when the fan started operating, pushing out heated air as soon as the outlet collector temperature exceeded 60 °C. At this point, the temperature stabilized somewhat, although the resistor continued to operate, causing a gradual temperature increase as long as solar radiation kept rising.

The temperature began to go up shortly after 10:00 AM, maintaining its upward trend all through the afternoon and reaching its highest point at the center.

The decline in temperature became noticeable during the time range of 1:30 PM to 3:00 PM, as solar radiation intensity decreased, transitioning from 890 to 518. This decrease followed a clear

linear trend, indicating a direct connection between diminishing solar radiation and the subsequent decrease in temperatures across the collector.

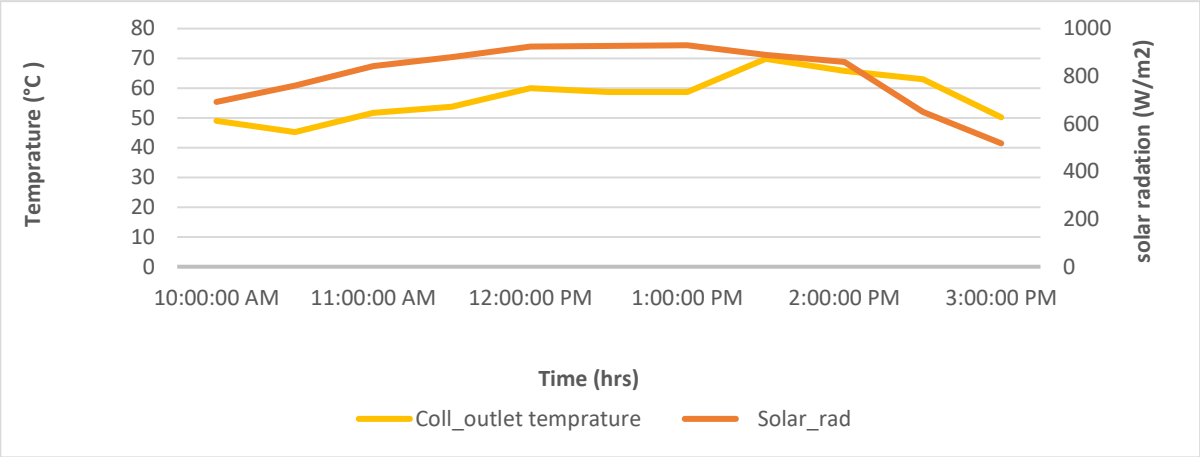

Figure 6.2. Variation of solar intensity and collector air temperature with time

6.3 VARIATION OF COLLECTOR TEMPERATURES WITH TIME FOR NO-LOAD TEST 2/21/2024

Figure 1 shows how the air temperature is heated as it passes over the collector. The collector Temp 1 undergoes a small rise from 12:00 PM to 1:00 PM, showing an increasing amount of solar radiation during this period. However, a small shift in behavior occurs between 1:00 PM and 1:30 PM, marked by intervals of decrease in temperature. This shift is attributed to sudden weather changes experienced during that timeframe, Notably, from 1:00 PM to 3:00 PM,

A crucial factor influencing the Collector Temp 1 is cloud cover, causing deviation immediately, as this temperature sensor is located outside of the collector.

Interestingly, other collector temperatures (Collector Temps 2, 3, and 4) continue to show a temperature increase, regardless of cloud cover. This phenomenon is linked to a heated resistor inside the collector, which retains heat and is consistently powered by a charged battery. Consequently, the collector's internal temperature (Collector Temps 2, 3, and 4) remains elevated. Also, the presence of a sand bed at the bottom of the collector plays a crucial role in increasing the Collector Temps of 2, 3, and 4. This sand bed acts as a reservoir, storing and releasing solar heat energy into the collector. Even during periods of low insolation, the accumulated heat in the gravel bed continues to discharge, contributing to the greenhouse effect inside the collector which makes the deviation in trend of the Collector Temp 1 from the Collector Temps 2, 3, and 4.

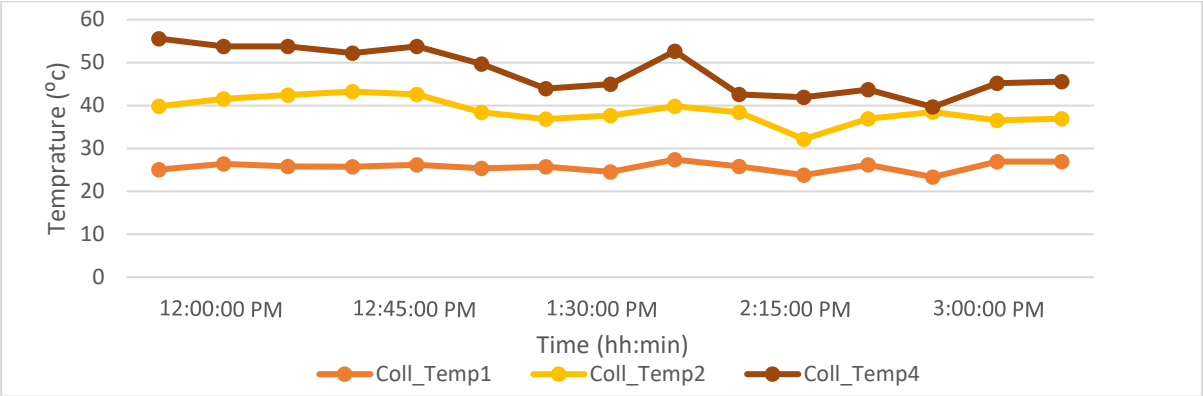

Figure 6.3. Variation of collector temperatures with time for no-load test for 2/21/2024

6.4 VARIATION OF ALL COLLECTOR AND TRAY TEMPERATURES WITH TIME FOR NO-LOAD TEST FOR 2/21/2024

The temperatures in Collector Temperature 4 are slightly higher first than those in the dryer tray temperatures (Drier_Temp 1, 2, 3, and 4) then it becomes almost similar to those tray temperatures. This is because hot air from the collector flows to the dryer, and along the way, it loses some heat to balance things out, after balance is attend, it is seen from the figure that the collector outlet temperature becomes similar with the other tray temperatures. In Abubakr's smart setup, each tray has its own chimney. This special design helps hot air travel directly from the collector to the trays, keeping temperatures similar. Also, there's a layer of fiberglass inside the dryer that acts like a warm blanket, preventing heat from escaping. Potential losses from holes and openings in the system may also contribute to temperature differences between the collector and dryer trays.

During the testing hours, the collector outlet air temperature and drying chamber temperatures displayed a greater range of variations compared to the ambient air temperature. This observation highlights the solar dryer's superior performance in contrast to conventional open-air sun drying methods. Notably, in a no-load test scenario, the solar dryer achieved an impressive maximum collector outlet air temperature of 55.59 °C at approximately 12 pm, coinciding with a corresponding solar insolation of 655 W/m^2 as shown in table 6.4 below:

when compared to the findings of (S Abubakar et al., 2018).In their study, the maximum collector outlet air temperatures for collectors with and without thermal storage materials during a no-load test were 66 °C and 53 °C, respectively. These temperatures were recorded alongside a solar insolation of 872 W/m^2. The discernible difference in temperatures underscores the

significant compression in performance offered by this solar dryer in comparison to the results reported by Abubaker et al., 2018.

Table 6.1. No load Temperature reading on February 21in °C

Time	Coll_ Temp1	Coll Temp 4	Coll_ Temp 4 - Coll_ Temp 1	Tray Temp 1	Tray Temp 2	Tray Temp 3	Tray Temp 4	Avg. Tray temp.
11:00:00 AM	22.2	47.76	25.56	37.78	37.17	36.96	38.6	37.62
11:30:00 AM	23.6	48.89	25.29	43.61	42.36	40.5	42.14	42.15
12:00:00 PM	25.1	55.59	30.49	45.14	44.17	42.58	43.82	43.92
12:30:00 PM	25.81	53.77	27.96	46.59	45.81	43.59	44.98	45.24
1:00:00 PM	26.16	53.77	27.61	46.37	45.69	44.4	44.75	45.30
1:30:00 PM	25.72	43.94	18.22	40.27	38.5	37.68	37.57	38.50
2:00:00 PM	27.41	52.63	25.22	46.94	45.57	43.59	44.51	45.15
2:30:00 PM	23.78	41.91	18.13	40.07	38.19	37.07	37.88	38.30
3:00:00 PM	23.34	39.65	16.31	38.07	36.76	36.06	36.66	36.88
3:30:00 PM	26.96	45.57	18.61	43.5	43.59	43.25	44.17	43.62
4:00:00 PM	24.92	43.25	18.33	41.81	41.8	41.48	41.8	41.72
Average	25	47.43	22.43	42.74	41.78	40.65	41.53	41.67

With this solar dryer, dryer elevate the ambient temperature by 30°C or even more. Referring to the data presented in the table, we observe that the maximum tray temperature reached was 46°C. Interestingly, a notable decrease in temperature is evident around 3 PM, attributed to the opening of the door at that particular time.

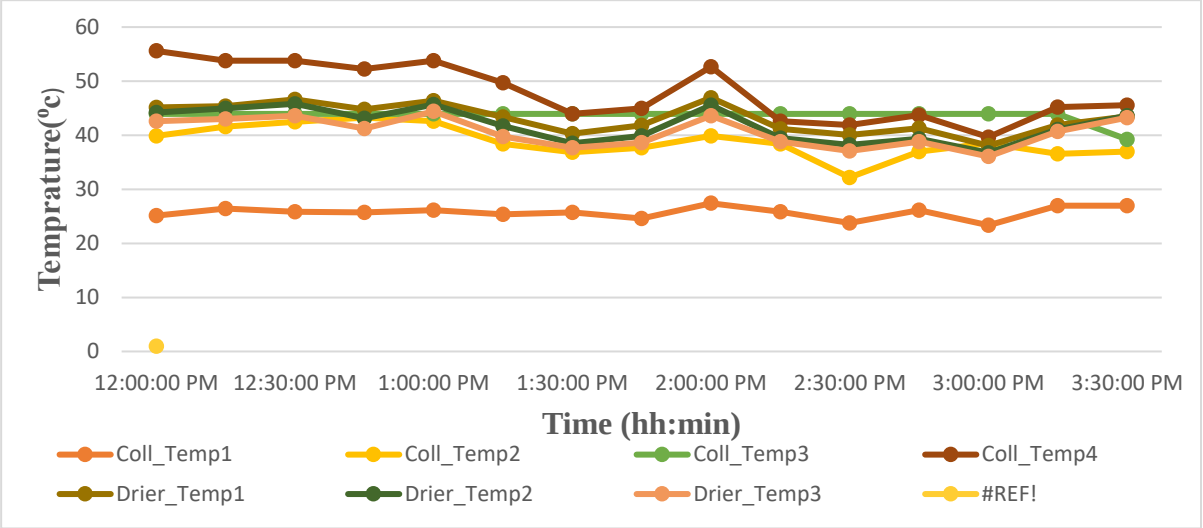

Figure 6.4. Variation of all collector and tray temperature with time for no load test 2/21/2024

6.5 VARIATION OF COLLECTOR INLET – OUTLET TEMPERATURES AND TRAY TEMPERATURES WITH TIME FOR NO-LOAD TEST FOR 2/20/2024

The temperatures are measured at specific locations denoted by Coll_Temp1, Coll_Temp2, Coll_Temp3, Coll_Temp4, Drier_Temp1, Drier_Temp2, Drier_Temp3, and Drier_Temp4 for both dryer without and with heater as sown in the figure 6.4 and 6.5. These figures provide insights into the thermal dynamics of the system over time recorded at different intervals throughout the day, spanning from 12:00 PM to 3:00 PM.

In considering the solar radiation levels and temperature differences recorded on February 20th without a heater and February 21st with a heater, we observe an interesting pattern. Despite the higher solar radiation recorded on February 20th (870 units) compared to February 21st (670 units), the temperature difference between ambient and collector temperatures is higher on February 21. On February 21st with the heater, the maximum temperature difference is 30 degrees Celsius, whereas on February 20^{th} without the heater, it is only 21 degrees Celsius. Additionally, the lowest tray temperatures observed, were 36.05 degrees Celsius with the heater and 33.71 degrees Celsius without the heater.

Tray temperatures in a solar dryer typically follow a pattern where they decrease from the bottom to the top, with Tray 1, closest to the collector, having the highest temperature. However, under no load conditions at noon in this experiment, we observed a small deviation from this expected trend. They may be because of the unique design of the solar dryer, shaped like a pyramid at the top, exposes the upper trays to intense noon sunlight from four sides, resulting

in higher temperatures at noon as shown in the figure bellow. Nonetheless, the data collected indicates that the temperatures across the four trays have only very small differences.

Most importantly, the fluctuations in the collector outlet air temperature and the drying chamber temperatures exceeded those of the surrounding ambient air temperature throughout the testing period. This observation suggests that the dryer has the capability to surpass traditional open-air sun drying methods

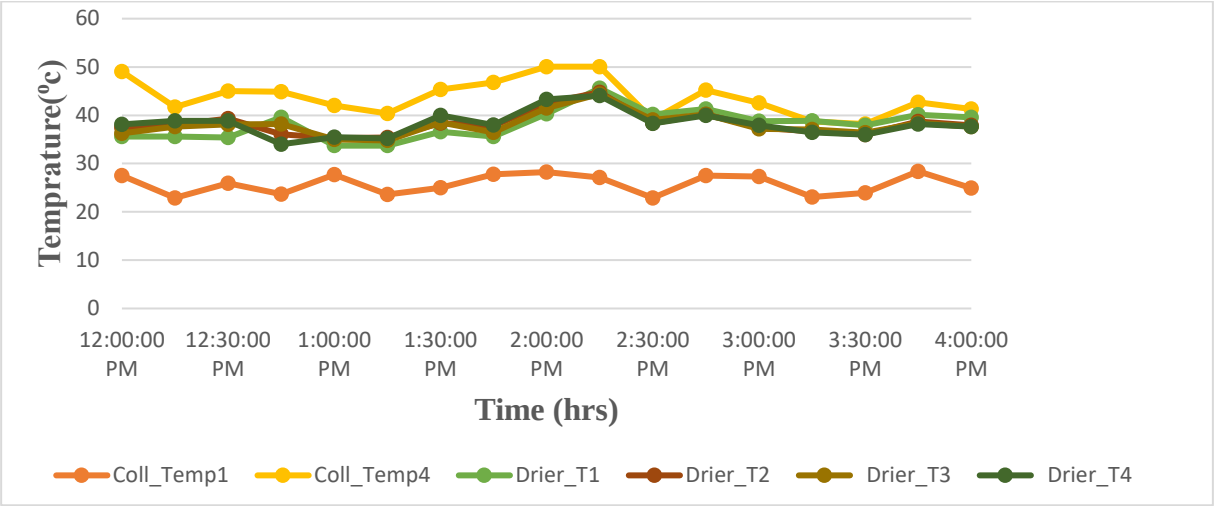

Figure 6.5. Variation temperatures with time for no-load test without heater for 2/20/2024

6.6 VARIATION OF OUTLET COLLECTOR AIR TEMPERATURE WITH TIME FOR FEBRUARY 20, 21/2024

The temperature is notably higher for the collector outlet temperature with the heater activated. This is attributed to the sustained operation of the resistor, which then warms up the surrounding air, leading to an increase in the overall temperature by drawing energy from the battery even in instances of low insolation

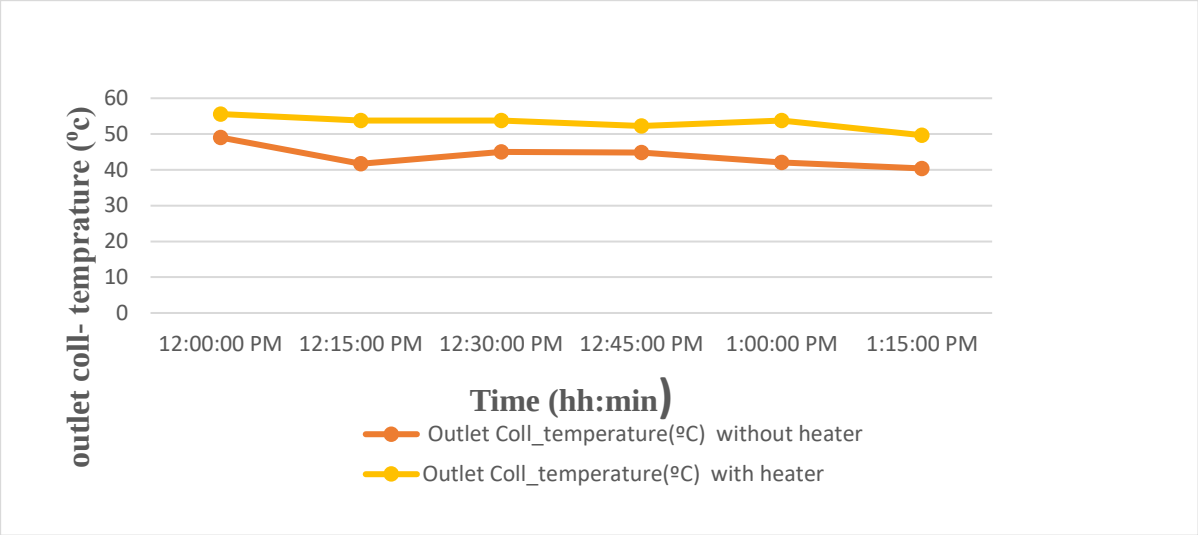

Figure 6.6. Variation of outlet collector air temperature with time for February 20, 21/2024

Figure 15 and figure 16 shown below Show the variation of solar insolation, ambient air temperature, collector air temperature for collector with and without heater with time for 21th and 20th February, 2024 respectively, at 01:00 PM with the heater and 12:00 PM without the heater, the measured maximum solar power to be 655 W/m² and 780 W/m² respectively. This shows we can get hotter air for drying things when there's more solar radiation. But surprisingly, the air was actually hotter at 01:00 PM with less solar radiation. This happened because only the resistor made the air hotter. And the resistor continues to generate heat, even when solar radiation is absent, because it receives power from the battery.

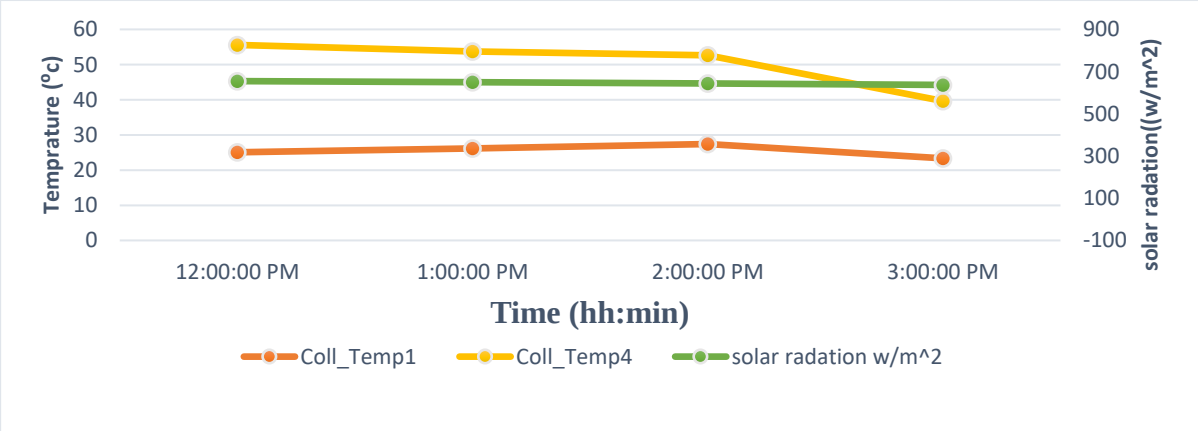

Figure 6.7. Variation of solar intensity, ambient air temperature and collector air temperature versus time with heater on for 2/21/2024

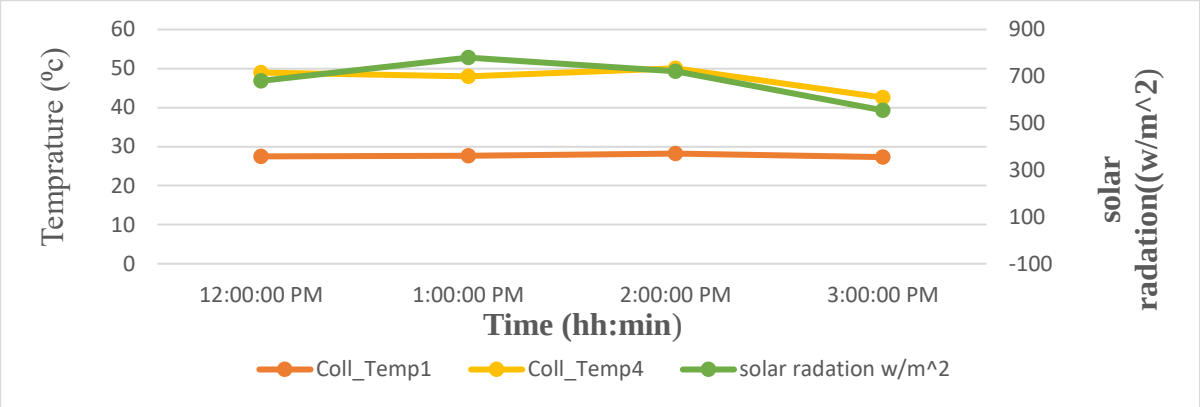

Figure 6.8. Variation of solar intensity, ambient air temperature and collector air temperature versus time with heater off for 2/20/2024.

6.7 Performance Evaluation Parameters

The weight variation after drying for about 20 hours in both the solar dryer with four trays and the open sun can be clearly observed in the figures presented below. These figures depict the significant impact of the drying method on the weight variation, and it is evident that the solar dryer with four trays outperforms the open sun tray in terms of weight or moisture variation.

Figure 6.9. Tray 1, 2, 3 moisture and weight reduction pictures after 20 houres

The table below illustrates the time and weight loss of red chili during the drying process across two methods, solar dryer (Tray 1, Tray 2, Tray 3, Tray 4) and open sun drying. Each entry shows the weight loss (in grams) from the initial weight of the red chili, providing insights into the effectiveness and efficiency of each drying method over the observed time periods. The data reveals notable variations in weight loss trends, emphasizing the importance of considering both time and method in optimizing the drying process for red chili.

Table 6.2. Comparison of Red Chili Weight Loss Across two Drying Method

Days	Time (hrs.)	Weight loss from red chili														
		Tray 1			**Tray 2**			**Tray 3**			**Tray 4**			**Open sun**		
		w_1	w_2	w_3	w_1	w_2	w_3	w_1	w_2	w_3	w_1	w_2	w_3	w_1	w_2	w_3
Feb 22 (2hr)	11:50 AM	14.9	12.4	10.2	17	9.8	16.2	16	17.9	12	12.8	12.1	13.5	12.9	20	13.5
	12:50 PM	14.6	12.1	10.0	16.7	9.3	16.1	15.8	17.5	11.7	12.6	12	13.4	12.5	20	13.3
	1:50 PM	14.3	11.8	9.8	16.4	9.2	15.7	15.6	17.2	11.6	12.4	11.5	13.2	12.5	19.8	13.2
Weight of water lost (g)		0.6	0.6	0.4	0.6	0.6	0.5	0.4	0.7	0.4	0.4	0.6	0.3	0.4	0.2	0.3
Feb 23 (6 hrs.)	11:10 AM	13.8	11.4	9.4	16.1	8.7	15.3	15	16.8	11.1	12.2	11.5	13	12.3	19.5	12.9
	1:10 PM	13.2	11	8.9	16.0	8.34	14.8	14.6	16.5	10.7	11.0	11	12.9	12	19	12.6

	3:10 PM	12.8	10.7	8.8	15.7	7.98	14.3	14.2	16	10.4	10.9	10.2	12.4	11.9	18.8	12.1
	4:10 PM	12.5	10.5	8.3	15.2	7.71	14.0	14	15.6	10.3	10.9	10	12	11.6	18.4	12
Weight of water lost (g)		1.8	1.3	1.5	1.2	1.49	1.7	1.4	1.6	1.3	1.5	1.5	1.5	0.9	1.4	1.2
Feb 24 (6 hrs.)	12:00 PM	11.7	9.9	7.8	14.2	7.1	13.3	13.3	14.6	9.7	10.5	10.5	11.6	10.9	17.8	11.5
	2:00 PM	10	9.5	7	13.9	6.6	12.6	12.7	14	9.2	10.2	9.5	11.2	10.5	17	11.1
	4:00 PM	8.9	8.9	6.8	13.2	6.2	11.9	12	13.4	8.7	10	9.01	10.4	10.2	16.5	10.74
Weight of water lost (g)		3.6	1.6	1.5	2	1.5	2	1.9	1.3	1.6	0.9	2.49	1.2	1.4	1.9	1.26
Feb 25 (2 hrs.)	3:30 PM	8.2	8.3	6.4	12.8	5.5	11.3	11.1	12.65	8.14	9.8	8.4	10.2	9.8	16.3	10.1
	4:30 PM	7.9	8.1	6.1	12.4	5.4	10.9	11	12.6	7.9	9.5	8.1	9.9	9.7	15.9	9.9
Weight of water lost (g)		1	0.8	0.7	0.8	0.8	1	1	0.85	0.7	0.5	0.9	0.9	0.5	0.6	0.7
Feb 26 (2 hr.)	2:00 PM	7.05	7.2	5	11.76	4.59	9.7	9.96	11.6	7.12	8.61	7.4	9.13	8.83	15.2	9.25

	3:30 PM	6.2	6.4	4.7	11	4	9.2	9.2	11	6.5	7.7	6.7	8.5	8.4	15	8.69
Weight of water lost (g)		1.7	1.7	1.4	1.36	1.3	1.7	1.8	1.6	1.4	1.8	1.4	1.4	1.3	0.8	1.21
Feb 27 (3hrs.)	10:30 PM	5	4.9	4.4	10.1	3.2	8.5	8.2	9.2	4.6	6.4	5.6	7.4	8	14.5	7.5
Weight of water lost(g)		1.2	1.5	0.3	0.9	0.8	0.7	1	1.8	1.9	1.3	1.1	1.1	0.4	0.5	1.19
Feb 28(3hrs)	10.30 PM	2.6	2.4	2.1	8.5	2	5.8	5.7	6.8	2.7	3.02	3.79	4.8	6.55	13.5	6.5
Weight of water lost(g)		2.4	2.5	2.3	1.6	1.2	2.7	2.5	2.4	1.9	3.38	1.81	2.6	1.45	1	1
Feb 29 (2hr)	2:30 PM	2.5	2.34	2	5.3	1.9	4.6	5.4	6.6	2.4	2.87	3.6	4.5	4	12.3	5.87
	Weight of water lost(g)	0.1	0.06	0.1	3.2	0.1	1.2	0.3	0.2	0.3	0.15	0.19	0.3	2.55	1.2	1.32

6.6.1 Weight loss of red chili

To investigate the mass and moisture loss in pepper samples subjected to both open sun and solar dryer methods, fresh pepper samples are carefully placed into four trays in the solar dryer and one tray to open sun, ensuring equal distribution for each drying method. Throughout the experiment, weight measurements are taken at hourly intervals to track the weight losses and moisture content calculations. An analytical weighting scale tool is used for these measurements, ensuring accurate data collection. After each measurement session, the pepper samples are attentively handled and placed into labeled plastic bags. This step is crucial for preserving the moisture content of the samples between measurement intervals and preventing any external moisture interference. Additionally, to maintain a controlled environment and prevent unintended moisture fluctuations from one day to the next, the samples are stored in a desiccator. The table shown below titled "Daily Moisture Loss of Red Chili on Drying Trays and Open Sun" indicates the daily weight loss of red chili peppers on drying sample trays having equal initial masses (tray 1 and tray 3) as well as the weight loss in the open sun over the specified duration from February 21st to February 29th

The table provides insights into the weight loss patterns of red chili during drying, employing two distinct methods: the dryer (Tray 1, Tray 3, and Tray 4) and open sun drying. Across all trays and durations observed, a consistent decrease in weight is evident, with weight differences ranging from 0.1 to 0.3 grams between Tray 1 and Tray 3 during drying. Specifically, while the dryer (representative of Tray 1,2) achieves notable weight reduction in approximately 24 hours, open sun drying demands more than days to achieve comparable results.

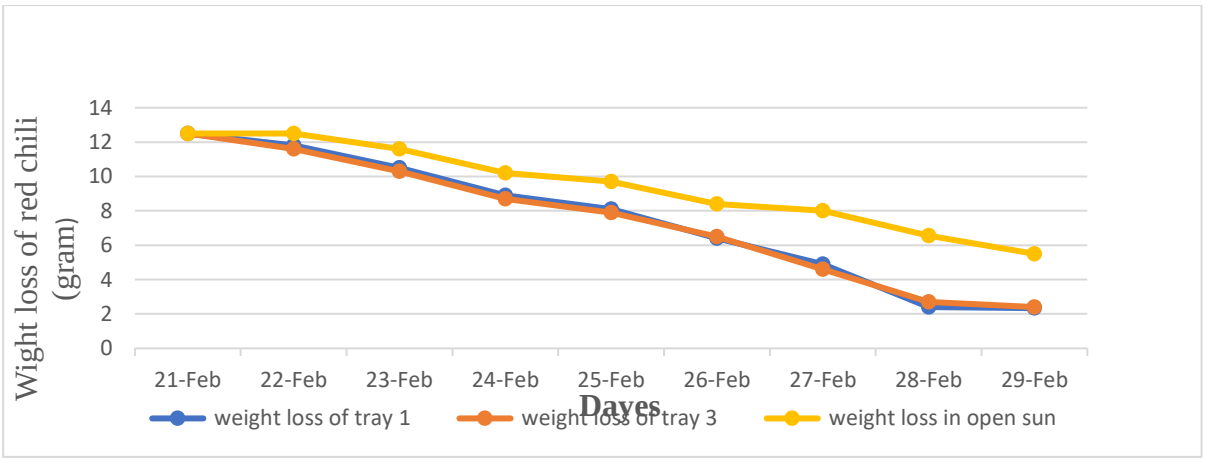

Figure 6.10. Weight Loss of red chili with Time

6.6.2 Moisture content

The data given in the table below represents the percentage moisture loss (wet basis) observed during the drying process of red chili using two different methods (solar dryer and open sun). Specifically, the graph illustrates the moisture loss trends for Tray 1, Tray 3, and open sun drying over a period spanning from February 21^{st} to February 29^{th}. This comparison sheds light on the effectiveness and efficiency of these drying methods in reducing the moisture content of red chili over time,

The results in the figure below illustrate that starting from an initial moisture content of 91%, it decreases to a safe level of 11% moisture content within a span of 26 hours. Notably, there wasn't a significant variance in moisture loss among trays within the dryer. However, compared to tray 1, there was a substantial 24% difference in moisture loss observed under open sun condition.

On February 21^{st}, at the start of our experiment, all situations had 0% moisture loss, meaning they were equally wet. As the days passed, the amount of moisture lost increased steadily.

When we compare how well Tray 1 and Tray 3 of our solar food dryer work compared to just leaving the chili out in the sun, we can see big differences. Tray 1 and Tray 3 consistently lost more moisture each day than the chili left in the sun. This shows that using the solar dryer helps in drying the chili faster than just relying on the sun.

By February 29^{th}, the end of our observation period, the difference was clear. Tray 1 and Tray 3 had lost much more moisture (81.28% and 80.80% respectively) compared to the chili left in the sun, which had only lost 56% of its moisture. This shows how effective the solar food dryer is at drying the chili quickly and thoroughly.

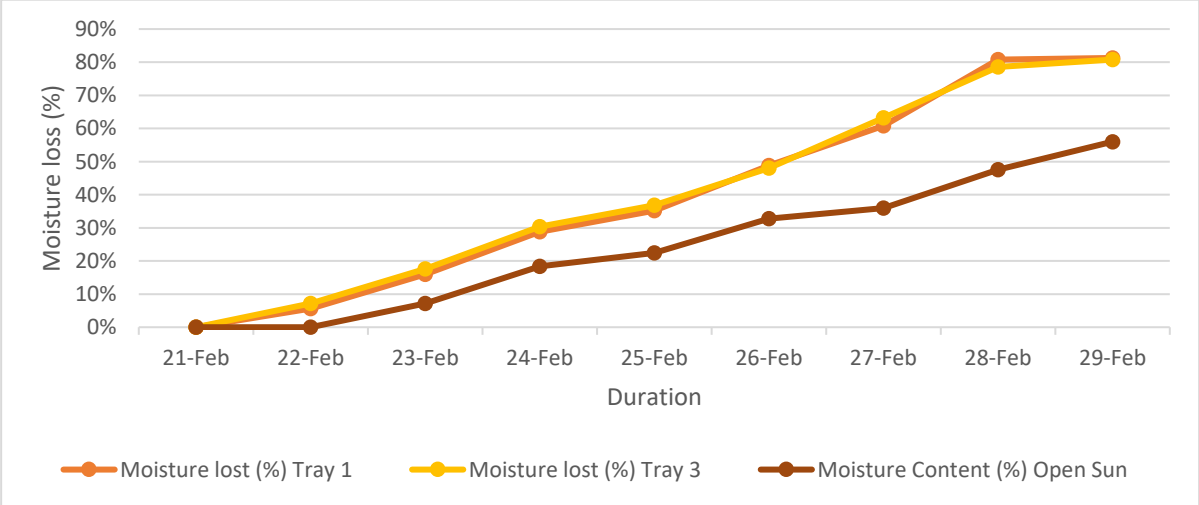

Figure 6.11. Moisture loss against day

6.6.3 Average drying rate

The drying rate represents the rate of change of moisture content (% w.b.) Over a particular time, interval and it can be expressed in % wb /min. Average drying rate, w_{dr} is determined from the mass of moisture to be removed by solar heat and drying time given in equation [3] above:

$$w_{dr} = \frac{m_r}{t_d}$$

The average drying rate of all trays, as shown in the figure, is notably higher than that observed in open sun conditions, which is at $0.997 \times 10^{-5} \frac{kg}{sec}$. Furthermore, the drying rate of red chili on four different trays inside the dryer exhibits almost identical values when compared to open sun drying. Initially, there was a rapid decrease in moisture content with time, which was seen on February 22 and 23. Subsequently, this process gradually slowed down from February 24 to Feb 26, eventually reaching a stage where saturation occurred from February 27 to 29.

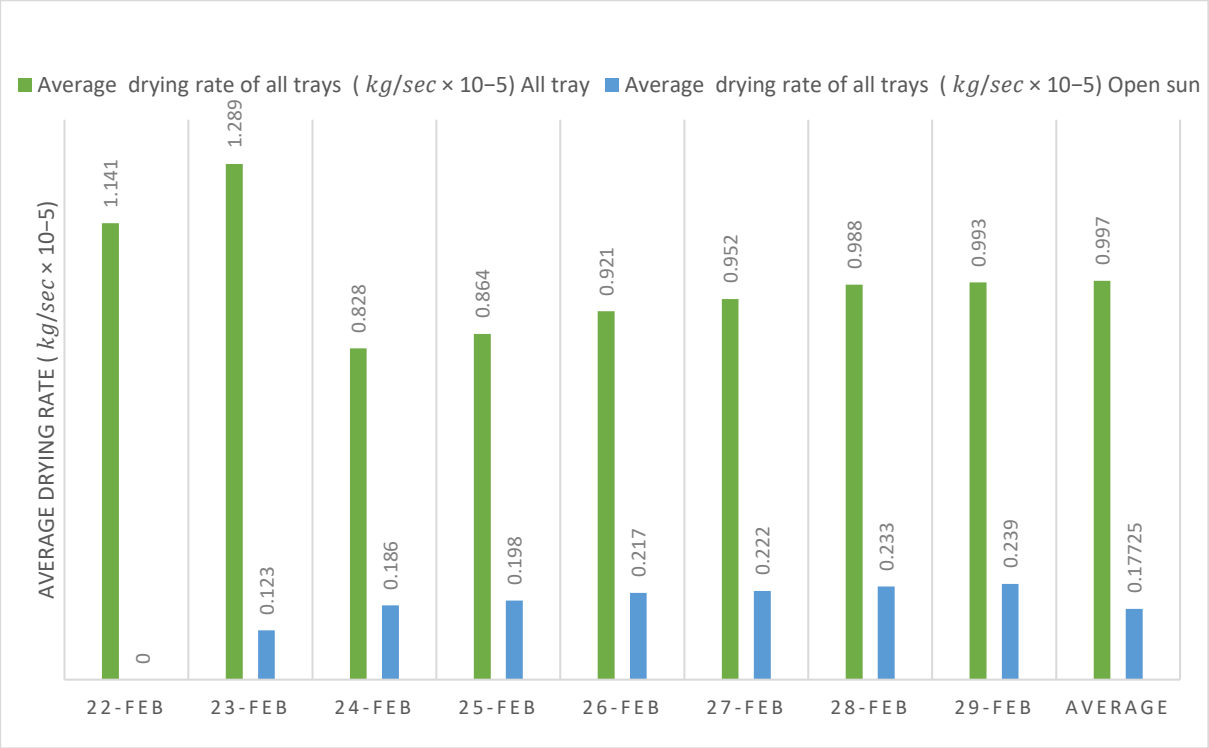

Figure 6.12.: Average drying rates for red chili

6.6.4 Collector efficiency

Figures 19 and 20 illustrate much better performance with collector and dryer efficiencies of 62% and 27%, respectively, as compared to the results reported by other researchers.

Murali (2019) reported a drying efficiency and collector efficiency of 23.81% and 46.26%, respectively. Fudholi (2013) obtained a collector efficiency of 28% and a dryer efficiency of 13%, while Mohanraj (2009) obtained an average dryer efficiency of 21%. Similarly, Zewdu (2021) reported drying and collector efficiencies of 22.6% and 15%, respectively, and Sileshi (2020) reported a collector efficiency of 30%. However, the results reported by Abubakar (2018) show somehow related performance with my work, with a collector and dryer efficiency of 67.25% and 28.75%, respectively even though they are not the same models. This is because the design allows hot air to flow directly from the collector to the trays, resulting in maximum heat transfer additionally, the dryer has a layer of fiberglass, which acts as a warm blanket, preventing heat from escaping and further enhancing its efficiency

To achieve an optimal design, an average collector efficiency of 40% was considered as a design parameter. However, the calculated collector efficiency shows an even better efficiency than the assumed value, which is 62% as shown in the collector efficiency calculation table.

Figure 6.13. Variation of collector efficiency with drying period

6.6.5 Dryer Efficiency (system efficiency)

It is the ratio of total amount of energy required to total amount of energy supplied to remove the moisture from the chili.

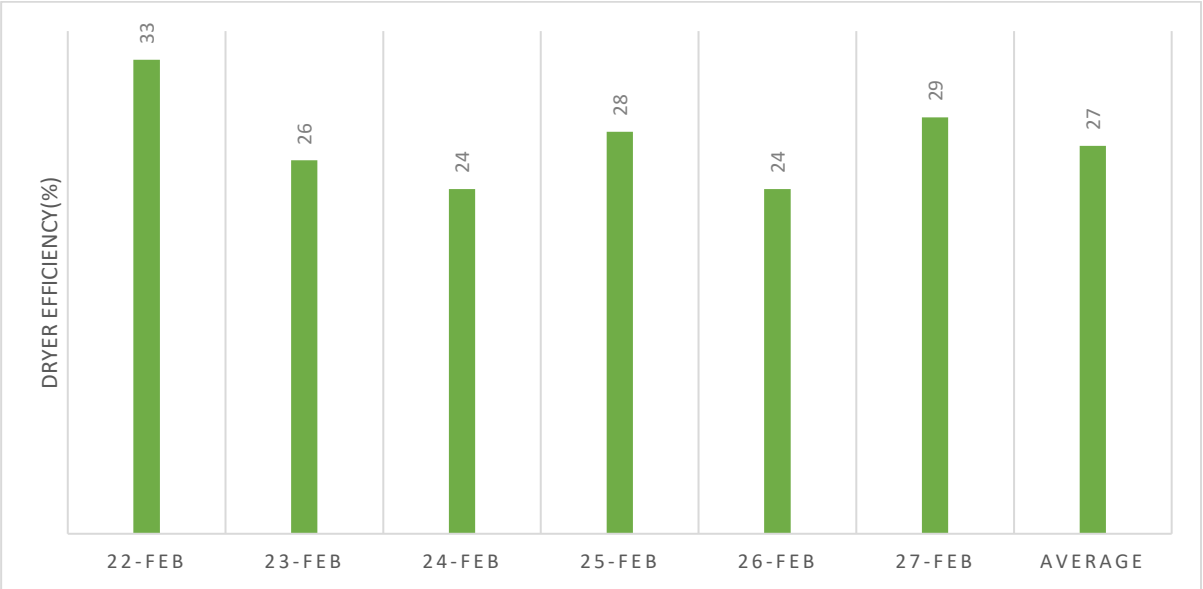

Figure 6.14. Variation of dryer efficiency with drying period

/

CHAPTER SEVEN
CONCLUSION AND RECOMMENDATIONS

7.1 CONCLUSION

Solar food dryers are an eco-friendly alternative to electrical food dryers. However, making them work like an oven has been a challenge because the fluctuating air temperature inside the solar food dryer have a negative impact on the quality of the food being dried. In an electrical food dryer, we can set the temperature to the exact required optimum temperature for a specific food item and maintain a constant temperature until the required amount of moisture is removed. To achieve this with solar food dryers, a constant temperature needs to be maintained at all times, even when solar radiation is low. In this work heater and fan are used to accomplish this task, heater receives a continuous flow of heat from the battery, which is charged by the solar PV cell. In case the heater is continuously charged and heated than the required optimum temperature. The temperature inside the dryer is controlled by a relay using an Arduino C++ code. Which maintains a constant temperature by turning the heating element and fan off and on as needed and the dryer generated heat is then circulated by fan. The hot air is distributed uniformly throughout the chamber, this ensures that the items inside the dryer are not over heated. This ensures that the temperature remains constant throughout the drying process, similar to that of an oven. This control mechanism avoids any unwanted temperature changes during the drying process.

This improved hybrid solar dryer system can be used to dry any type of food item with an optimum temperature lower than 55°C. And for those higher optimum drying temperature requiring food items, the size of the resistor and Solar Power System Components can be improved accordingly. This red chili dryer was designed using the meteorological conditions of Addis Ababa, Ethiopia. With Maximum collector outlet air temperature of 55.5 °C @ 655 w/ $m^2$and 50.06 °C @ 722 w/ m^2 respectively for the collector with and without heater under no load conditions.

The performances of this drying systems were evaluated using the percentage moisture loss, drying rate, collector efficiency and drying efficiency. The solar food dryer utilized to dry the chili took a total of 26 hours to reduce the moisture content from an initial moisture content of 91% to the final desired moisture content of 10%, 11%, 13%, 14%, and 35% for tray 1, tray 2, tray 3, tray 4, and open sun, respectively. And the average drying rates, average collector

efficiency, and average drying efficiency of the drying system with heater are 0.997 $\times 10^{-5}\ \frac{kg}{sec}$, 62.3%, and 27% respectively. The improved hybrid solar dryer system offers better control mechanisms, ensuring that the temperature inside the dryer remains constant and doesn't affect the quality of the food being dried. It is a highly effective system that can be used for a wide range of food items.

7.2 RECOMMENDATION

- Upgrade the size of the resistor and solar power system components to support higher optimal drying temperatures. This enhances flexibility, enabling the system to accommodate a variety of food items with different temperature requirements since system has adjustable temperature control systems.
- The performance evaluation of the dryer should encompass day and night cycles, particularly due to the presence of sand storage material. This is critical as both the heat generated by the heating element and the solar radiation contribute to substantial stored energy.
- conduct thin layer drying models to enhance the understanding of the drying process. Additionally, color and pungency tests should be performed to assess the quality of the dried food items it is also crucial for optimizing the efficiency and quality of the drying process.

MANUFACTURING DRAWING OF IMPROVED HYBRID SOLAR DRYER

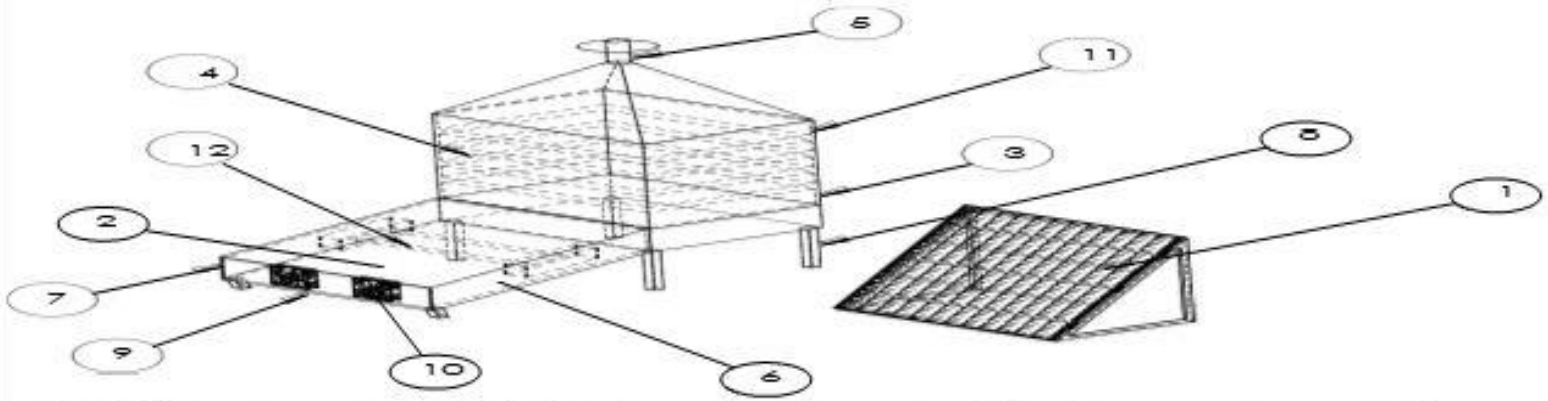

ITEM NO.	PART NUMBER	Drawing Number.	QTY.
1	PV CELL	DEI-IHSD-000/23	1
2	SOLAR COLLECTOR	DEI-IHSD-002/23	1
3	DRYING CHAMBER	DEI-IHSD-005/23	1
4	ROCKSOR TRY	DEI-IHSD-004/23	4
5	CHIMNEY	DEI-IHSD-005/23	1
6	ABSORBER	DEI-IHSD-003/23	1
7	SAND BED	DEI-IHSD-009/23	1
8	LEG	DEI-IHSD-006/23	6
9	COLLECTOR	DEI-IHSD-002/23	1
10	FAN	DEI-IHSD-000/23	2
11	DOOR	DEI-IHSD-010/23	1
12	HEATER	DEI-IHSD-000/23	1

ALL DIMENSIONS ARE IN MILLIMETERS

	NAME	SIGNATURE	DATE	TITLE:
DRAWN BY	HELEN WORKU			DESIGN AND EXPERIMENTAL INVESTIGATION OF IMPROVED HYBRID SOLAR DRYER
CHK'D BY	KAMIL DINO (PHD)			
APPV'D BY				

MATERIAL: | DWG NO. DEI-IHSD-001/23 | A4

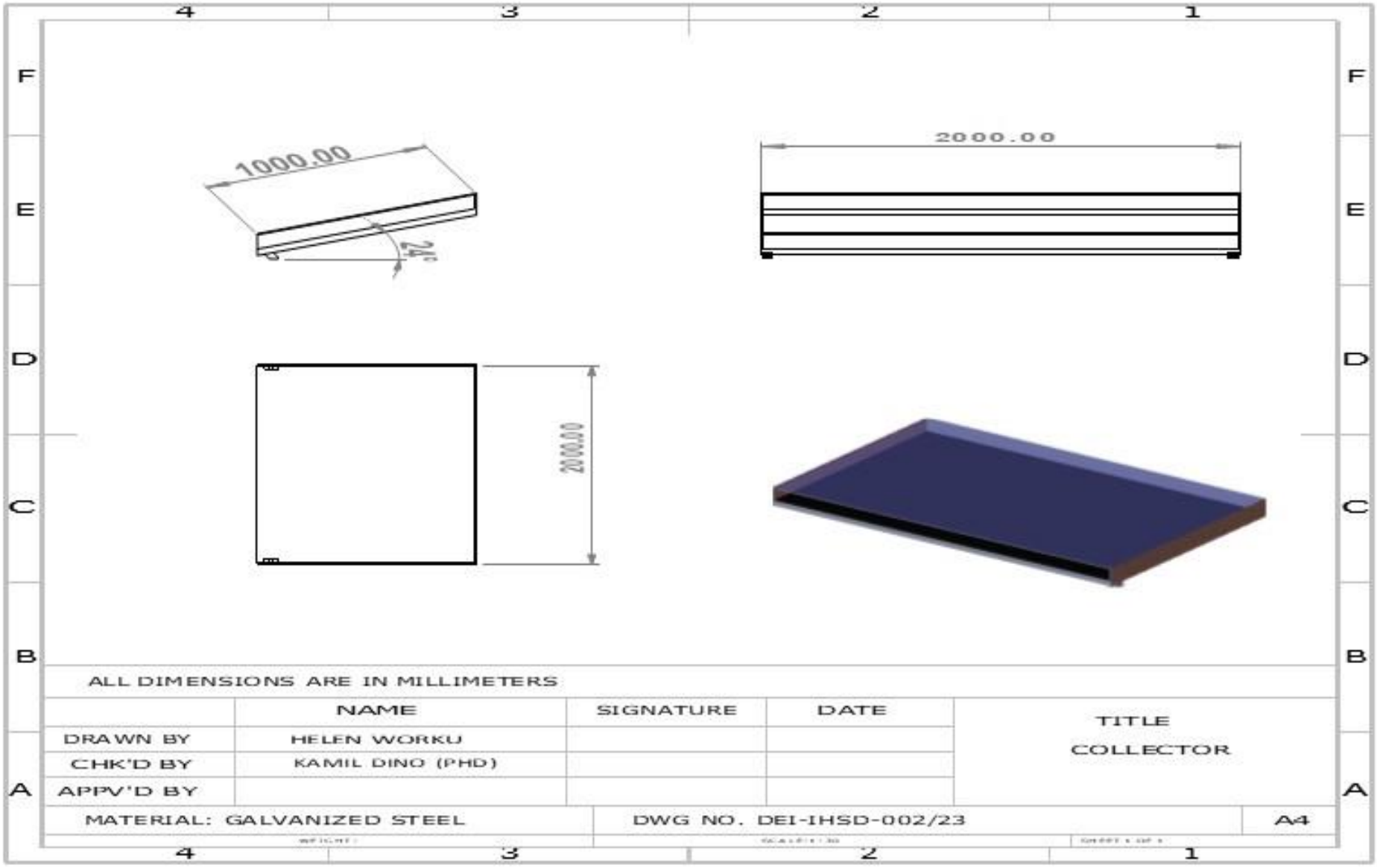
4
3
2
1
F
E
D
C
B
A
1000.00
24°
2000.00
2000.00
ALL DIMENSIONS ARE IN MILLIMETERS
NAME
SIGNATURE
DATE
TITLE
DRAWN BY
HELEN WORKU
CHK'D BY
KAMIL DINO (PHD)
APPV'D BY
COLLECTOR
MATERIAL: GALVANIZED STEEL
DWG NO. DEI-IHSD-002/23
A4

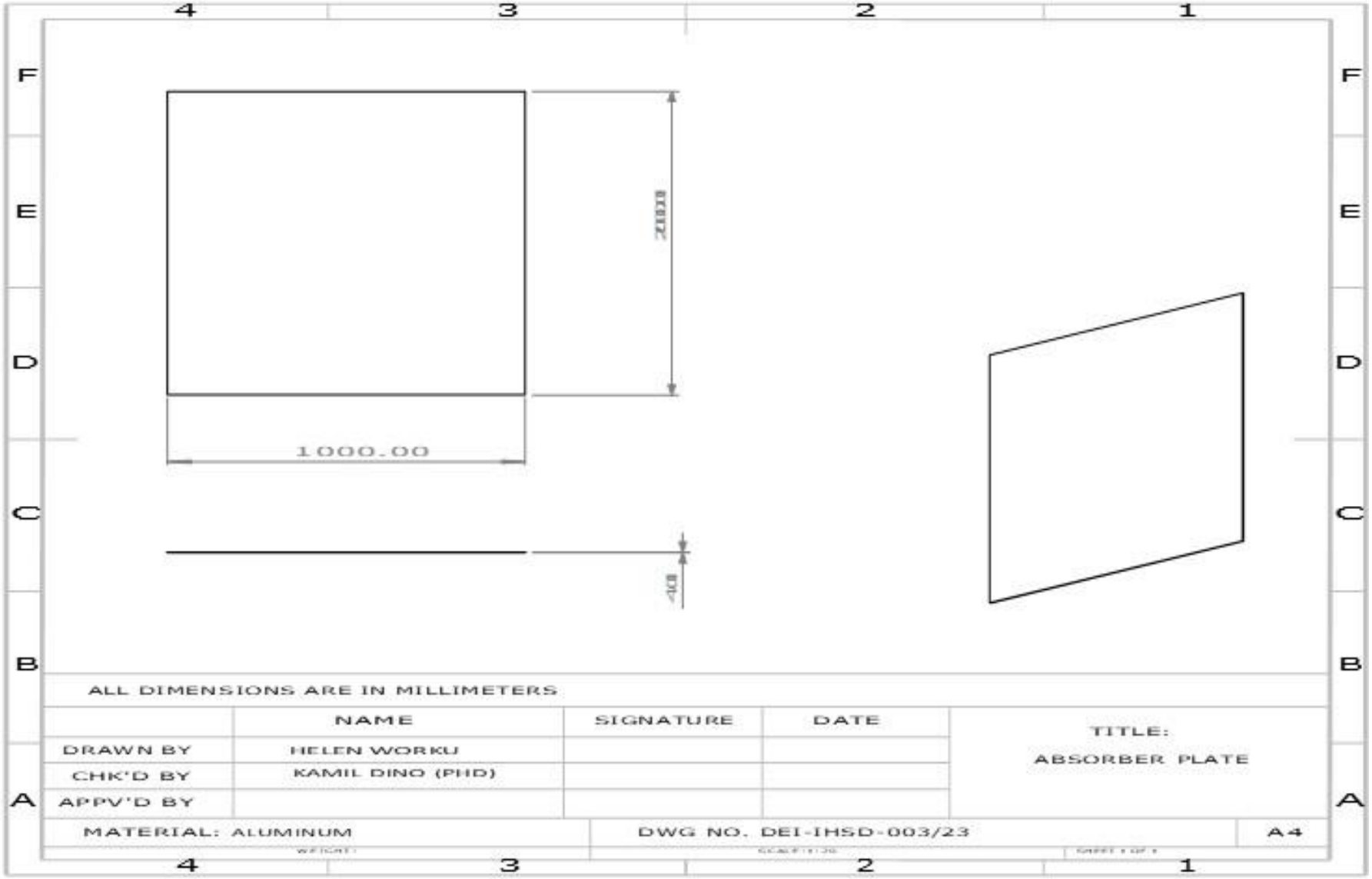
4
3
2
1
F
E
D
C
B
A
2000
1000.00
40
ALL DIMENSIONS ARE IN MILLIMETERS
NAME
SIGNATURE
DATE
TITLE:
ABSORBER PLATE
DRAWN BY
HELEN WORKU
CHK'D BY
KAMIL DINO (PHD)
APPV'D BY
MATERIAL: ALUMINUM
DWG NO. DEI-IHSD-003/23
A4

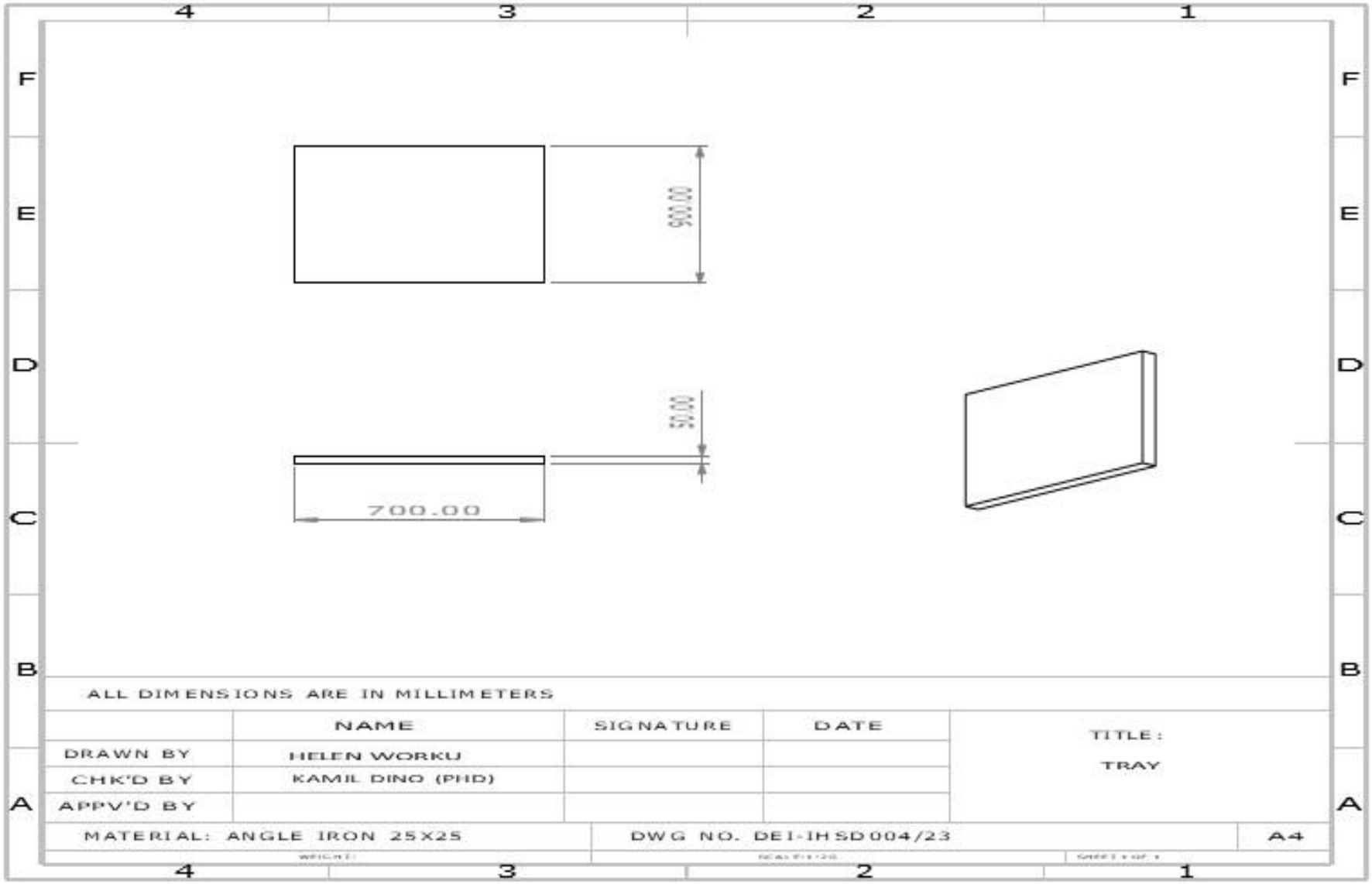
4
3
2
1
F
E
D
C
B
A
900.00
50.00
700.00
ALL DIMENSIONS ARE IN MILLIMETERS
NAME
SIGNATURE
DATE
TITLE:
TRAY
DRAWN BY
HELEN WORKU
CHK'D BY
KAMIL DINO (PHD)
APPV'D BY
MATERIAL: ANGLE IRON 25X25
DWG NO. DEI-IHSD004/23
A4

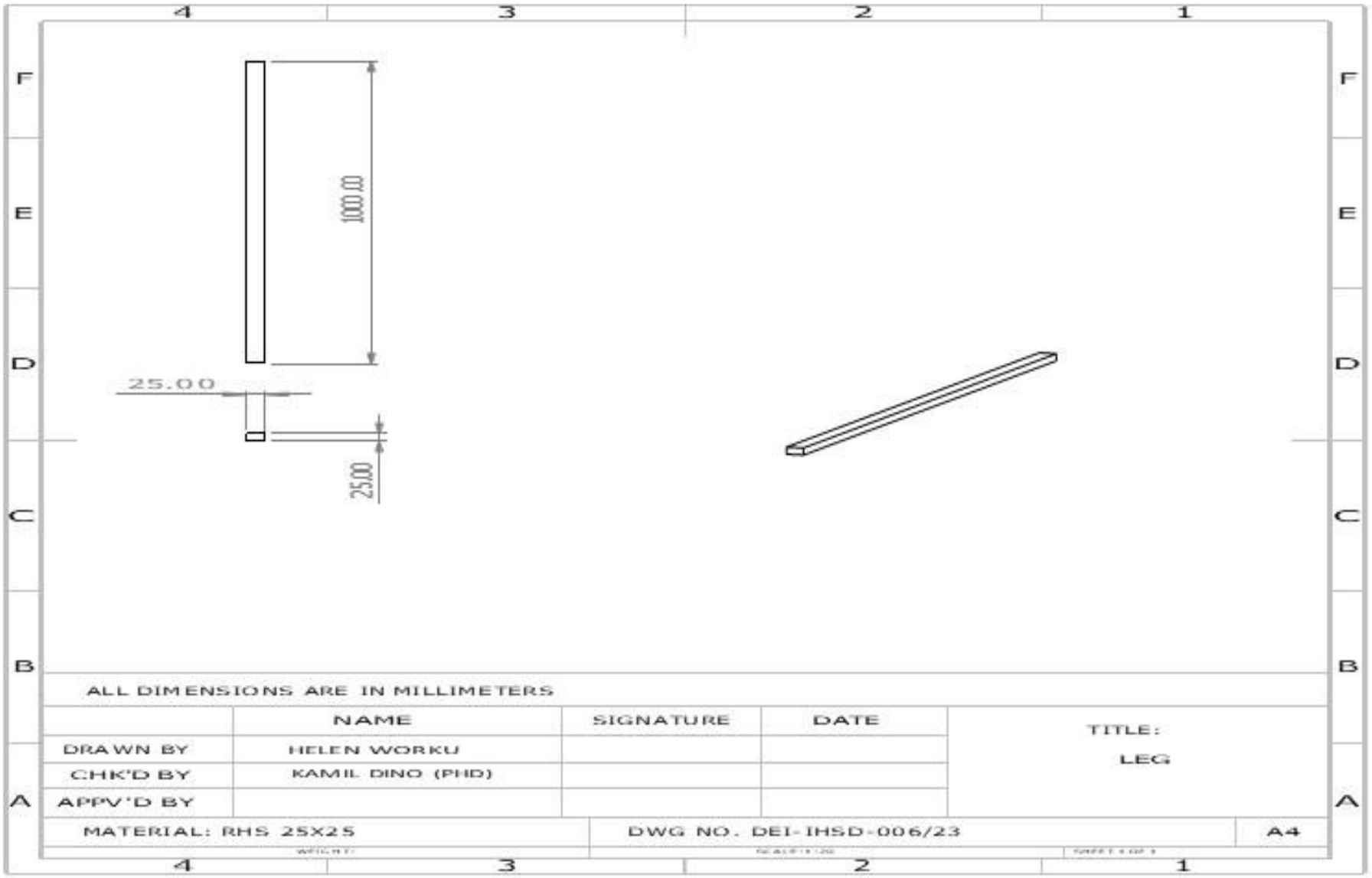
4
3
2
1
F
E
D
C
B
A
1000.00
25.00
25.00
ALL DIMENSIONS ARE IN MILLIMETERS
NAME
SIGNATURE
DATE
TITLE:
LEG
DRAWN BY
HELEN WORKU
CHK'D BY
KAMIL DINO (PHD)
APPV'D BY
MATERIAL: RHS 25X25
DWG NO. DEI-IHSD-006/23
A4

REFERENCE

Abubakar, S., Umaru, S., Kaisan, M. U., Umar, U. A., Ashok, B., & Nanthagopal, K. (2018). Development and performance comparison of mixed-mode solar crop dryers with and without thermal storage. *Renewable Energy, 128*, 285-298. doi:10.1016/j.renene.2018.05.049

Admass, Z., Salau, A. O., Mhari, B., & Tefera, E. (2024). Red pepper drying with a double pass solar air heater integrated with aluminium cans. *Scientific Reports, 14*(1). doi:10.1038/s41598-024-53563-6

Afzal, A., Iqbal, T., Ikram, K., Anjum, M. N., Umair, M., Azam, M., . . . Majeed, F. (2023). Development of a hybrid mixed-mode solar dryer for product drying. *Heliyon, 9*(3). doi:10.1016/j.heliyon.2023.e14144

Alemayehu, H. (2019). Comparative Experimental Investigation between Parabolic Dish and Flat Plate Collector based solar dryer for saw dust briquette production.

Amer, B. M., Gottschalk, K., & Hossain, M. (2022). Corrigendum to: Integrated hybrid solar drying system and its drying kinetics of chamomile [Renewable Energy 121 (2018)– 539-547]. *Renewable Energy, 182*, 1241.

Banout, J., et al. (2011). Design and performance evaluation of a Double-pass solar drier for drying of red chilli (Capsicum annum L.). *Solar Energy, 85*(3), 506-515. doi:https://doi.org/10.1016/j.solener.2010.12.017

Dursun, E. (2021). Solar Energy Potential in Horn of Africa: A Comparative Study Using Matlab/Simulink. *Balkan Journal of Electrical and Computer Engineering, 9*(3), 310-319.

Eltawil, M. A., Azam, M. M., & Alghannam, A. O. (2018a). Energy analysis of hybrid solar tunnel dryer with PV system and solar collector for drying mint (MenthaViridis). *Journal of Cleaner Production, 181*, 352-364. doi:10.1016/j.jclepro.2018.01.229

Eltawil, M. A., Azam, M. M., & Alghannam, A. O. (2018b). Solar PV powered mixed-mode tunnel dryer for drying potato chips. *Renewable Energy, 116*, 594-605. doi:10.1016/j.renene.2017.10.007

Forson, F. K. (1999). Modelling and experimental investigation of a mixed-mode natural convection solar crop dryer (MNCSD).

Fterich, M., Chouikhi, H., Elloumi, A., Bentaher, H., Maalej, A., & Hamza, E. PERFORMANCE OF AN AGRO-FOOD SOLAR DRYER EQUIPPED WITH A PV/T AIR COLLECTOR.

Getahun, E., Delele, M. A., Gabbiye, N., Fanta, S. W., & Vanierschot, M. (2021). Studying the drying characteristics and quality attributes of chili pepper at different maturity stages: experimental and mechanistic model. *Case Studies in Thermal Engineering, 26*, 101052.

Getahun, E., Gabbiye, N., Delele, M. A., Fanta, S. W., Gebrehiwot, M. G., & Vanierschot, M. (2020). Effect of maturity on the moisture sorption isotherm of chili pepper (Mareko Fana variety). *Heliyon, 6*(8).

Holman, J. P. (1986). *Heat transfer*: McGraw Hill.

Hossain, M. Z., Hossain, M., Awal, M. A., Alam, M. M., & Rabbani, A. (2015). Design and development of solar dryer for chilli drying. *International Journal of Research, 2*(1), 63-78.

Hussein, J., Hassan, M., Kareem, S., & Filli, K. (2017). Design, construction and testing of a hybrid photovoltaic (PV) solar dryer. *environment, 1*(5), 1-14. M.A. Hossain a, B.K. Bala b. (2007). Drying of hot chilli using solar tunnel drierdoi:10.1016/j.solener.2006.06.008

Mohammed, S. A., Alawee, W. H., Chaichan, M. T., Abdul-Zahra, A. S., Fayad, M. A., & Aljuwaya, T. M. (2024). Optimized solar food dryer with varied air heater designs. *Case Studies in Thermal Engineering, 53*. doi:10.1016/j.csite.2023.103961

Mohana, Y., Mohanapriya, R., Anukiruthika, T., Yoha, K., Moses, J., & Anandharamakrishnan, C. (2020). Solar dryers for food applications: Concepts, designs, and recent advances. *Solar Energy, 208*, 321-344.

mohanraj1, p.chandrasekar2. . (2009). performace of a forced convection solar drier integrated with gravle as heat storage material for chili drying. *4*(3), 305 - 314.

Murali, S., Amulya, P., Alfiya, P., Delfiya, D. A., & Samuel, M. P. (2020). Design and performance evaluation of solar-LPG hybrid dryer for drying of shrimps. *Renewable Energy, 147*, 2417-2428.

Murali, S., Sathish Kumar, K., Alfiya, P., Delfiya, D. A., & Samuel, M. P. (2019). Drying kinetics and quality characteristics of Indian mackerel (Rastrelliger kanagurta) in solar–electrical hybrid dryer. *Journal of Aquatic Food Product Technology, 28*(5), 541-554.

Musa B. Ibrahim1, A. M., Haruna Abubakar3. (2016). Development of a Solar Powered Standing Dc Fan Using Three Phase. *American Journal of Engineering Research (AJER, 5*(12), 148-154.

Oloketuyi S Idowu*, O. M. O. a. O. I. I. (2013). Determination of optimum tilt angles for solar collectors in low-latitude tropical region. *nternational Journal of Energy and Environmental Engineering*.

Paul, B., & Singh, S. (2013). Design, development and performance evaluation of solar dryer with mirror booster for red chilli (capsicum annum). *International Journal of Engineering Trends and Technology, 5*(1), 25-31.

Salih, A. R. (2023). Seasonal Optimum Tilt Angle of Solar Panels for 100 Cities in the World. *Al-Mustansiriyah Journal of Science, 34*(1), 104-110. doi:10.23851/mjs.v34i1.1250

Scanlin, D. (1997). Indirect, through-pass, solar food dryer. *Home Power. February*.

Scanlin, D. (1999). The Design, Construction, and Use of anIndirect, Through-Pass, Solar Food Dryer. 34.

Shrivastava, V., Kumar, A., & Baredar, P. (2014). Developments in indirect solar dryer: a review. *International Journal of Wind and Renewable Energy, 3*(4), 67-74.

Sileshi, S. T. (2014). *Design and Manufacturing of Solar Injera Dryer.* Addis Ababa,

Sileshi, S. T., Hassen, A. A., & Adem, K. D. (2021). Drying kinetics of dried injera (dirkosh) using a mixed-mode solar dryer. *Cogent Engineering, 8*(1), 1956870.

Sileshi, S. T., Hassen, A. A., & Adem, K. D. (2022). Simulation of mixed-mode solar dryer with vertical air distribution channel. *Heliyon, 8*(11).

Stephen, A. K., & Emmanuel, S. (2009). Improvement on the design of a cabinet grain dryer. *American Journal of Engineering and Applied Sciences, 2*(1), 217-228.

Tesema, S., & Bekele, G. (2014). Resource assessment and optimization study of efficient type hybrid power system for electrification of rural district in Ethiopia. *International Journal of Energy and Power Engineering, 3*(6), 331-340.

teshome, s. (2020). *Design and Manufacturing of Solar Injera Dryer.* (B.Sc.).

Vengsungnle, P., Jongpluempiti, J., Srichat, A., Wiriyasart, S., & Naphon, P. (2020). Thermal performance of the photovoltaic–ventilated mixed mode greenhouse solar dryer with automatic closed loop control for Ganoderma drying. *Case Studies in Thermal Engineering, 21*, 100659.

Zemedkun, B. (2021). *Mathematical Modeling and Simulation of Mixed Mode Natural Convection Solar Dryer for Green Banana Flour Production.* (B.Sc.). Addis Ababa

Zewdu, M. Z. (2021). *Design, Manufacturing and Performance Evaluation of Modified Solar Bubble Dryer for Pepper-Vegetable Crop.* (masters). Addis Ababa

APPENDIX: TABLES

- **Raw data from testes of daily weight loss of red chili on drying trays and open sun:**

Duration	Weight reduction of tray 1 (gram)	Weight loss of tray 3 (gram)	Weight loss in open sun(gram)
21-Feb	12.4	12	12.5
22-Feb	11.8	11.6	12.5
23-Feb	10.5	10.3	11.6
24-Feb	8.9	8.7	10.2
25-Feb	8.1	7.9	9.7
26-Feb	6.4	6.5	8.4
27-Feb	4.9	4.6	8
28-Feb	2.4	2.7	6.55
29-Feb	2.34	2.4	5.5

- **Raw data from testes of daily % moisture loss of red chili on drying trays and open sun:**

Duration	Percentage Moisture loss (wet basis (%) tray 1	Percentage Moisture loss (wet basis (%) tray 3	Percentage Moisture loss (wet basis (%)) open sun
21-Feb	0	0	0
22-Feb	5.60	7.2	0
23-Feb	16	17.60	7.20
24-Feb	28.80	30.40	18.40
25-Feb	35.20	36.80	22.40
26-Feb	48.80	48	32.80
27-Feb	60.80	63.20	36
28-Feb	80.8	78.40	47.60
29-Feb	81.28	80.80	56

- **Calculated data for average drying rate for red chili:**

Day	Average drying rate ($kg\ /sec \times 10{-}5$)					
	Tray 1	Tray 2	Tray 3	Tray 4	All tray	Open sun
February 22	0.114	0.088	0.085	0.854	1.141	0
February 23	0.77	0.169	0.173	0.177	1.289	0.123
February 24	0.211	0.208	0.21	0.199	0.828	0.186
February 25	0.22	0.218	0.22	0.206	0.864	0.198
February 26	0.234	0.229	0.232	0.226	0.921	0.217
February 27	0.242	0.233	0.242	0.235	0.952	0.222
February 28	0.249	0.243	0.248	0.248	0.988	0.233
February 29	0.25	0.246	0.249	0.248	0.993	0.239
Average	0.28625	0.20425	0.207375	0.299125	0.997	0.17725

- **Calculated collector efficiency raw data table:**

Day	Solar radiation (w/m^2)	T_a [k]	T_0 [k]	$T_0 - T_a$ [k]	c_p [J/kg. K]	A_c m^2]	ṁ [$\frac{kg}{s}$]	ṁ *c_p * ^T	A_c*I [w]	μ_c (%)
21-Feb	584	298	326	27.96	1005	2	0.026	730.5	1168	62.5
22-Feb	437	297	325	28.27	1005	2	0.026	738.6	874	84.5
23-Feb	584	301	328	27.18	1005	2	0.026	710.2	1168	60.8
24-Feb	648	304	329	25.78	1005	2	0.026	673.6	1296	51.9
25-Feb	535	300	326	26.39	1005	2	0.026	689.5	1070	64.4
26-Feb	650	304	329	24.72	1005	2	0.026	645.9	1300	49.6
Avg.	573	300	327	27.11	1005	2	0.026	698.1	1146	62.3

- **Calculated drying efficiency table:**

Day	I[w/$\boldsymbol{m^2}$]	μ_d
22-Feb	437	33
23-Feb	584	26
24-Feb	648	24
25-Feb	535	28
26-Feb	650	24
27-Feb	524	29
Average	563	27

- **Technical Parameters of charge controller:**

Model	KT1205	KT1210	KT1215	KT1220
Rated charging current	5A	10A	15A	20A
Rated discharging current	5A	10A	15A	20A
Short-current protection	25A	25A	25A	25A
System voltage	12V/24V Auto adapt			
Over current protection	<1.3 maintain for 60s			
	<1.6 maintain for 5s			
	>1.6 shut down immediately			
Stand-by lost	<5mA			
Charge voltage drop	≤0.26V			
Discharge voltage drop	≤0.15V			
Max solar panel voltage	21V			
Operating temperature	-35ºC to +55ºC			
Equalize charging voltage	14.8V			
Bulk charging voltage	14.5V			
Acceptance charging voltage	14.2V			
Float charging	13.8V			
Charge return voltage	13.2V			
Discharge stop voltage	11.2V			
Discharge return voltage	12.6V			
Temperature compensation	N/C			
Control mode	PWM (Pulse Width Modulation)			
Maximum wire size	12AWG			
	140×90.5×28.5mm/210g			